Spring 2009

Factors Promoting Variation in Feeding Morphology of Larval Southern Toads (Bufo Terrestris)

Matthew C. Schacht

FACTORS PROMOTING VARIATION IN FEEDING MORPHOLOGY OF LARVAL SOUTHERN TOADS (*Bufo terrestris*)

by

MATTHEW C. SCHACHT

Under the direction of Lance McBrayer

ABSTRACT

Larval anurans exhibit morphological plasticity in response to environmental conditions. However, the effect of the environment on morphological traits associated with feeding has been understudied. The purpose of this study was to: 1) determine if diet composition and feeding behavior affect chondrocranial morphology and denticle length of Southern toads (*Bufo terrestris*) in a laboratory setting, and 2) evaluate the potential for light intensity to affect chondrocranial morphology, denticle length, size, and developmental time of *B. terrestris* raised in three different shade environments. Linear and geometric morphometrics were used to quantify chondrocranial morphology for a group of specimens representing a range of ontogenetic stages, and for prometamorphic specimens as well. The results of this study indicate that diet (directly) and shade (indirectly) influence chondrocranial shape and denticle length.

INDEX WORDS: Southern Toad, Chondrocranium, Morphology, Plasticity

FACTORS PROMOTING VARIATION IN FEEDING MORPHOLOGY OF LARVAL SOUTHERN TOADS (*Bufo terrestris*)

by

MATTHEW C. SCHACHT

B.S., Huntingdon College 2006

A Thesis Submitted to the Graduate Faculty of Georgia Southern University in Partial Fulfillment of the Requirements for the Degree

MASTER OF SCIENCE

STATESBORO, GA

2009

FACTORS PROMOTING VARIATION IN FEEDING MORPHOLOGY OF LARVAL SOUTHERN TOADS (*Bufo terrestris*)

by

MATTHEW C. SCHACHT

Major Professor: Lance McBrayer

Committee: Ray Chandler
David Rostal
Risa Cohen

Electronic Version Approved:
May 2009

Dedication

For my parents, Eric and Joan Schacht, whose endless support and encouragement made this possible. Thank you for all you have given me, for always being there for me, for teaching me to always do my best, and most of all, for your unconditional love.

Acknowledgments

I would like to thank my advisor, Dr. Lance McBrayer, for his invaluable guidance, support, and friendship during my time at Georgia Southern University. I would also like to thank my committee, Dr. Ray Chandler, Dr. Risa Cohen, and Dr. David Rostal for their helpful guidance and advice. I thank my fellow graduate students Tim Gowan, Steve Williams, Jennifer O'Conner, and Nabil Nasseri, for their advice, support, and friendship. Finally, I thank my parents Eric and Joan Schacht for their tremendous support and encouragement throughout my academic career.

This research was approved by the Georgia Southern University IACUC, and funded in part by a Georgia Southern Graduate Student Professional Development Grant and a Georgia Southern University Academic Excellence Award.

TABLE OF CONTENTS

Page

LIST OF TABLES

Page

LIST OF FIGURES

PAGE

Chapter 1

Diet-induced morphological variation in larval Southern toads (*Bufo terrestris*)

Introduction

Intraspecific variation in diet preference and in methods of obtaining resources occurs in foragers from a wide range of taxa (insects, gastropods, fishes, birds) (Trowbridge 1991). Interestingly, this variation in diet and feeding behavior often produces morphological variation. Indeed, diet-induced morphological variation has been documented in multiple taxa (e.g. fishes and insects; Bernays 1986; Wainwright et al. 1991; Thompson 1992) and has been shown to occur in a variety of ways. For example, the texture of the foods consumed can lead to differential wear of feeding structures (Swennen et al. 1983) or increased development of jaw musculature used for feeding (Bernays 1986; Wainwright et al. 1991; Thompson 1992). Moreover, diet appears to be especially important in early development, as it may influence phenotypes to such an extent that divergent ontogenetic trajectories may be discerned for sympatric conspecifics (Trowbridge 1997).

Many species of larval anurans are known to use two different feeding behaviors, when consuming either planktonic material from the water column or benthic organic material from sediments and submerged substrates (Hoff et al. 1999). Larvae consuming planktonic material feed by filtering the suspended particles (Larson and Reilly 2003). In contrast, to consume benthic organic matter larvae must first generate a suspension that can be filtered by rasping or scraping the material using their keratinized beaks and labial teeth (Larson and Reilly 2003). Little is known concerning the proportion of time larval anuran species feed by filtering suspension versus time spent rasping and then filtering.

However, it is likely that the relative abundances and quality of available food types ultimately determine which feeding behavior is optimal at a given point in time. Thus, environmental variation in resource availability and quality probably promotes intraspecific variation in feeding behavior.

Individual variation in feeding behavior may result in morphological variation because the muscular mechanics involved in these feeding behaviors are highly dissimilar. In both fish (Wainwright et al. 1991; Mittelbach et al. 1992) and insects (Bernays 1986; Thompson 1992), jaw musculature has been shown to be correlated with food type and texture. Bernays (1986), showed that as diet increased in hardness, caterpillars of the noctuid *Pseudalatia unipuncta* developed larger and more robust heads with greater surface area for attachment of the mandibular muscles. Wainwright et al. (1991) showed that pumpkinseed sunfish (*Lepomis gibbosus*) in lakes where snails were abundant possessed larger pharyngeal jaw muscles than those from a lake depauperate in snails. Larval anurans may respond to diet composition in a similar manner. Individuals that feed primarily by rasping may develop more robust chondrocrania with larger attachment sites for the muscles used during rasping (e.g. orbitohyoideus, hyoangularis, and suspesorioangularis). In contrast, larval anurans that feed primarily by filtering suspension may allocate resources towards increasing buccal volume, which allows for greater volumes of water to be filtered.

As feeding behavior influences jaw musculature, subsequent morphological changes in structures that function as muscular attachment sites may occur. In larval anurans, the cartilaginous chondrocranium supports the jaw apparatus and serves as an attachment site for many of the muscles involved in feeding (Larson 2002). Fine scale

variation in chondrocranial shape may be an artifact of variation in jaw musculature. This may be especially true because the resultant forces of muscular contractions have been shown to influence the morphology of primary cartilage (Herring 1993).

In addition to chondrocranial morphology, diet composition and feeding behavior may also elicit a plastic response in mouth width. Larval leopard frogs (*Rana* pipiens) and wood frogs (*Rana sylvatica*) grow significantly wider mouths (measured as length of the longest denticle row) in response to competition (Relyea 2000; Relyea and Auld 2005). A wider denticle row enhances foraging efficiency by providing a larger surface area to rasp substrates for food, thereby enhancing an individual's ability to adaptively respond to competition (Relyea 2000). Denticle length plasticity might also be an adaptive response to variation in feeding behavior. For example, a large denticle would only enhance the foraging efficiency of individuals that feed primarily by rasping. Because the foraging efficiency of individuals that feed primarily by filtering suspension is unrelated to denticle length, the resources necessary to grow and maintain a large denticle might be used more effectively if they were allocated elsewhere. In circumstances where competition is negligible and an individual either demonstrates a clear preference for one feeding behavior over another, or environmental conditions favor one feeding behavior over another, plasticity in denticle length could function as way of enhancing the efficiency of resource utilization.

The goal of this study was to evaluate the effects of feeding behavior (filtering vs. rasping) on chondrocranial morphology and denticle length in larval Southern toads (*Bufo terrestris*) exposed to two diet treatments. Several methods were used to quantify and evaluate chondrocranial morphology across diet treatments: 1) scaling relationships

of the chondrocranial cartilages were discerned, 2) measurements of chondrocranial elements associated with muscles involved in feeding were compared across treatments, and 3) geometric morphometric methods were used to quantitatively compare morphology across treatments, both at later developmental stages (36+, Gosner 1960) and throughout ontogeny.

Materials and Methods

Experimental Design

Southern toad (*Bufo terrestris*) tadpoles were used as the focal organism for this study. Because this species is reportedly indiscriminate when selecting egg deposition sites (Gibbons and Semlitsch 1991), larvae can potentially encounter a wide variety of environmental conditions (canopy closure, resource quantity and quality, etc.). Larvae typically reach metamorphosis 30-55 days after hatching (Ashton and Ashton 1988).

To isolate the effects of dietary treatments, all tadpoles used in this experiment were full siblings, thus preventing any confounding results due to gross genetic dissimilarities. Full siblings were obtained by collecting a single pair of adult Southern toads in amplexus. This pair was returned to the laboratory for egg deposition. Following hatching, tadpoles (n = 350) were placed in 14 plastic tubs (37.3 x 21.6 x 12.7 cm) filled with 6 liters of aged water that was aerated for the duration of the experiment. Tadpoles were raised in laboratory conditions and subjected to one of two diet treatments (175 tadpoles/treatment). I randomly assigned tadpoles to plastic tubs at a density of 25 tadpoles per tub (~ 4 tadpoles/liter). At this density, it is unlikely that there were any adverse effects of crowding given the small size of Southern toad tadpoles (6.5-11 mm at metamorphosis, Ashton and Ashton 1988), the high densities at which they naturally

occur (personal observation; Wright and Wright 1949), and the periodic removal of individuals for analysis throughout the duration of this experiment. The experiment began on June 16, 2007 and was terminated September 4, 2007. The laboratory was on a 14:10 (L:D) photoperiod and all tadpoles were maintained between 21 and 23° C.

Each plastic tub was assigned either a suspension feeding treatment (n = 7) or rasping feeding (n = 7). I fed tadpoles in the suspension feeding treatment a mixture of finely ground tadpole food (frog and tadpole bites; HBH Enterprises, Springville, UT) and phytoplankton (*Chlorophyta vulgaris*) *ad libitum*. This mixture remained in suspension when the air supply in the plastic tubs was turned off; once food was added to the tubs tadpoles could clearly be seen swimming throughout the water column near the suspended particles (presumably suspension feeding). Rasping and scraping of the surfaces of the plastic tubs by tadpoles from the suspension feeding treatment was rarely observed, and each tub was vacuumed and cleaned every 2-3 days to prevent any food from settling on the bottom or sides of the containers. Throughout the experiment, algal growth on the sides or bottom of the containers used for the filtering treatment was never observed. The tadpoles subjected to the rasping treatment were fed algae growing on 10.16 cm^2 ceramic tiles. In order to obtain tiles with periphyton communities growing on them, I placed tiles in a local pond in Bulloch County, GA for a period of 30 days. I personally observed both *B. terrestris* larvae, and calling adults, at this pond on several occasions; therefore, the periphyton that was collected on the tiles and used in this treatment is representative of periphyton communities that larvae might potentially encounter in nature. Throughout the duration of the experiment each plastic tub contained two tiles, which were replaced with new tiles (heavily covered with algae, e.g.

>75% of the surface area was covered) when the amount of algae growing on them was noticeably reduced (approximately every 3-5 days).

Specimen Removal and External Morphology

I periodically removed and euthanized tadpoles in order to obtain multiple specimens from each treatment at developmental stages 28-38 (Gosner 1960). Following euthanization, each specimen's developmental stage and mass (after blotting with a paper towel) were recorded, and specimens were stored in 10% buffered formalin (Lindzey et al. 2002) until morphological measurements were taken. A total of 132 specimens (66 per treatment) were digitally photographed in a lateral view and snout-vent length (SVL; Fig 1A) measurements for all specimens were obtained from the photographs using TpsDig v. 1.18 (Rohlf, 1998, Department of Ecology and Evolution, SUNY, Stony Brook). The length of the longest denticle row (Fig 1B) on each specimen was measured using a dissecting scope fitted with an ocular micrometer.

Preliminary analysis indicated that no added variation due to tub was present (ANOVA: Log_{10} SVL x treatment, $F_{12}= 0.79$, $p= 0.66$); therefore, data for all specimens within each treatment were pooled for analysis. All morphological measurements taken in this study were log_{10} transformed to meet the assumptions of normality and homogeneity of variance. To determine if size (SVL) differed across treatments or developmental stage, I conducted an analysis of covariance (ANCOVA) with Gosner (1960) stage as the covariate. The Gosner stage x treatment interaction was not significant ($F_1 = 2.378$; $p = 0.125$) and was subsequently removed from analysis. In order to test the effect of treatment on denticle length, denticle length was regressed against SVL and collected the residuals to remove the influence of body size variation in denticle

length. Analysis of variance (ANOVA) was used to test for differences in residual denticle lengths among diet treatment groups.

Linear Morphometrics

To allow for linear and geometric morphometric comparisons of chondrocranial shape across treatments all 132 specimens were cleared and stained for cartilage and bone following the procedures described by Dingerkus and Uhler (1977). Dorsal views of the chondrocrania of all specimens were photographed with a digital camera. A total of 12 linear measurements (Figure 2; Table 1) from each specimen were obtained using TpsDig v. 1.18 (Rohlf, 1998, Department of Ecology and Evolution, SUNY, Stony Brook). Linear measurements were chosen following the criteria used by Larson (2002, 2004, 2005). The measurements used in this study describe the general shape of the chondrocranium (e.g., braincase length), as well as the shape of functionally important structures (e.g., muscular insertion sites such as the palatoquadrate and muscular process) (Larson 2002).

Reduced major axes regressions of each of the 12 $\log_{10}$-transformed chondrocranial measurements on $\log_{10}$ SVL were used to obtain regression slopes describing the scaling relationships of the linear measurements (Gould 1966, Harvey and Pagel 1991, Birch 1999). To test the null hypothesis of isometric scaling, 95% confidence intervals were calculated for the reduced major axes regression slopes. Given that the independent and dependant variables are length measurements, a value of $k = 1$ indicates isometric scaling. Thus, if confidence intervals fail to overlap a value of 1, the null hypothesis of isometry is rejected, confidence intervals greater than, or less than, 1 indicate positive allometry (CI >1) and negative allometry (CI <1). This methodology

was chosen because the independent and dependant variables are measured with error, therefore, ordinary least-squares regression would tend to underestimate the true slope of the relationship between independent and dependant variables (Harvey and Pagel 1991).

After evaluating allometric scaling patterns, I regressed linear measurements of the chondrocranium that are structurally important in feeding (THL, PAQO, THW, PAQL, SRA, EPW, MPW, CAW) against corresponding individual sizes (SVL). I then conducted one-way ANOVA's on the residual scores to test for differences across treatments. This was done to provide a more comprehensive evaluation of the effects of diet on feeding morphology, because allometric scaling patterns do not necessarily indicate size differences across treatments.

Geometric Morphometrics

Geometric morphometric methodology was used to determine if late-stage specimens from different diet treatments possessed discernable differences in chondrocranial morphology (hereafter termed: Terminal Shape Analysis, Larson 2005), and to determine if those differences were present throughout ontogeny (hereafter termed Whole Ontogeny Analysis, Larson 2005). For geometric morphometric comparisons of chondrocranial shape, a total of 11 landmarks (Fig. 3) were digitized on the right side of the chondrocranium of 32 specimens (for terminal shape analysis 16/treatment) and all 132 specimens (for whole ontogeny analysis, 66/treatment) using TpsDig v. 1.18 (Rohlf, 1998, Department of Ecology and Evolution, SUNY, Stony Brook). Following Larson (2005), I regressed SVL against Gosner stage, which produced a plot where SVL had clearly reached a plateau at a Gosner stage of 36, therefore only specimens from stage 36 and above were used in terminal shape analysis. Landmarks were chosen based on their

ability to represent the entirety of geometric form, and to describe functionally important structures (Larson 2002, 2004, 2005). The landmarks used in this study represent the tips or corners of processes, intersections of tissues, or points of maximum curvature (Table 2).

Landmark data were analyzed using geometric morphometric methodology. The procedures for obtaining geometric morphometric data are discussed in extensive detail elsewhere (Bookstein 1991; Rholf 1993; Rholf et al. 1996; Montiero 1999) and will only be briefly reviewed here. In short, landmark configurations for each specimen are scaled to unit centroid size and aligned to produce a consensus configuration (Larson 2002). The matrix of interlandmark distances of the consensus form is used to produce a set of eigen vectors known as principal warps, from which each specimen is projected to yield partial warp scores that can be used in statistical analysis (Bookstein 1991; Monteiro and Abe 1999; Larson 2002).

Landmark data for all specimens were analyzed using two approaches. First, relative warps analysis (RWA) was used to quantify variation in the landmark data. Relative warp analysis generates partial warp scores (n = 16 for this study; number of partial warps = 2p- 6; where p is the number of landmarks) and two uniform components. Thin-plate spline deformation grids depicting chondrocranial shape change at both positive and negative extremes along the first relative warp axis were obtained in order to enhance visual interpretation of morphological data. Finally, the partial warp scores and uniform components [calculated using Bookstein's (1996) linearized procrustes estimate in tpsRelw v. 1.18; Rohlf 1998] obtained from the landmark data were subject to

canonical variates analysis to determine if specimens could be correctly classified to their respective diet treatments based on chondrocranial shape.

Results

Body Size & Denticle Length

There was no effect of diet treatment on SVL (ANCOVA: F= 2.88; p= 0.092), and there was no significant effect of the interaction between diet treatment and Gosner (1960) stage (ANCOVA: F= 0.2.37; p= 0.125). Thus the results of the ANCOVA support the null hypothesis of homogeneity of slopes. Gosner (1960) stage did have a significant effect on SVL (F= 346.81; p= <.0001), however, this is not surprising, given that tadpoles grow throughout development. Tadpoles from the rasping diet treatment had significantly greater denticle lengths than those from the filtering treatment (ANOVA: $df_{1,131}$; F= 6.96; p= 0.0093).

Linear Morphometrics

The regression slopes indicated that specimens from the two diet treatments exhibited different allometric scaling patterns in four of the twelve chondrocranial elements measured in this study (PAQO, CAW, MW, and BCL; Table 3 and Table 4). The majority of the chondrocranial elements measured in specimens from the filtering treatment exhibited isometric scaling; only otic capsule length (OCL) and the distance between the braincase and the most lateral margin of the subocular bar of the palatoquadrate (BCPQ) scaled with negative allometry. In contrast, specimens from the rasping treatment exhibited an even mixture of isometry (PAQL, THL, SRA, THW, EPW, MPW) and negative allometry (PAQO, CAW, BCPQ, MW, OCL, BCL). In specimens from the rasping treatment, each of the chondrocranial elements posterior to

the muscular process of the palatoquadrate scaled with negative allometry, whereas only two posterior elements (BCPQ and OCL) scaled with negative allometry in specimens from the filtering treatment. Specimens from the rasping treatment had significantly greater values for five of the eight measurements that are structurally associated with feeding (Table 5). Although specimens from both treatments exhibited isometric scaling for PAQL, SRA, EPW, THW and MPW, these measurements were significantly greater in specimens from the rasping treatment. There was no difference in trabecular horn length (THL) across treatments, and the distance between the lateral articular processes of the palatoquadrate cartilages (PAQO), and the distance between the lateral margins of the ceratohyal articular facets just behind the hyoquadrate processes (CAW) was significantly greater in specimens from the filtering treatment.

Geometric Morphometrics (Whole Ontogeny)

Thin-plate spline deformation grids depicting chondrocranial shape change (relative to the consensus form) at positive and negative extremes along the first and second relative warp axes are shown in Figure 4. Together the first two axes explained 40.65% of the variation in the dataset. The first relative warp axis (RW1) explains variance in the spatial configurations of landmarks 4 through 8. When compared to the consensus configuration, the positive extreme of the first relative warp axis (RW1+) shows an increase in the distances between landmarks 4-5, a decrease in the distance between landmarks 6-7, and landmarks 7-8 are slightly anterior to their positions on the consensus form. In contrast, at the negative extreme (RW1-), the spatial changes in landmark positions are the inverse of RW1+ (distance between landmarks 4-5 decreases, 6-7 increases, and 7-8 move posteriorly). Therefore, the specimens with high RW1

scores possess a prominent muscular process (distance between landmarks 4 and 5) and a compressed orbit (landmarks 6,7, and 8), and specimens with low RW1 scores possess the opposite. The second relative warp axis (RW2) is characterized by a lateral expansion of landmarks 3-6 at the positive extreme (RW2+) and lateral compression of landmarks 3-6 at the negative extreme (RW2-). Also, RW2+ shows the position of landmark 9 as medial to the consensus form, whereas RW2- shows a lateral shift of landmark 9. Specimens with high scores on RW2 possess a chondrocranium with wider anterolateral margins, whereas specimens with low RW2 scores have narrower anterolateral margins.

Geometric Morphometrics (Terminal Shape)

Thin-plate spline deformation grids depicting chondrocranial shape at positive and negative extremes along the first two axes are shown in Figure 5. The results of the terminal shape analysis are similar to those from the whole ontogeny dataset, in that the spatial configurations of landmarks 3-8 seem to be the main source of variation in shape. At the positive extreme of RW1, landmark 3 is medial to its location on the consensus form, the distance between 4 and 5 has increased, and both 5 and 6 appear to have shifted in a posterolateral direction. The negative extreme (RW1-) shows the exact opposite. The extremes on RW2 depict changes in the spatial orientation of landmarks 1, 4, 5, 6, 7, and 8. At the positive end (RW2+) landmark 1 is posterior to its location on the consensus form, landmark 4 is medial, 5 is lateral, and the distance between 4-5 has increased. Also, the distance between 6-7, and 6-8 has decreased. Again, the negative extreme (RW2-) shows the exact opposite.

Geometric Morphometrics (CVA)

Results of the whole ontogeny CVA indicate significant differences in chondrocranial shape across treatments (Wilks'-Lambda: $F_{18,113}$= 4.78, p= < 0.0001). Of the 132 specimens, 84% (n = 111) were correctly classified to their respective diet treatment based on chondrocranial shape data alone. Specimens from the rasping treatment tended to score higher on the CV1 axes than those from the filtering treatment (Fig. 6).

The results from the CVA of terminal shape suggest that the degree of divergence in chondrocranial shape was more pronounced in late-stage specimens (36+). Terminal shape was significantly different across treatments (Wilks'-Lambda: $F_{18,13}$= 3.16, p= 0.01) and 97% of the specimens used in the terminal shape analysis were correctly classified to their respective diet treatment (1 specimen from the filtering treatment was misclassified). As with the whole ontogeny CVA, specimens from the rasping treatment scored higher on the first CV axis (Fig. 7).

Discussion

Denticle Length

This study is the first to document a plastic response of denticle length in larval *Bufo terrestris*. Previous studies have shown denticle length to be a plastic response to competition in *Rana sylvatica* (Relyea 2000, Relyea and Auld 2005) and *R. pipiens* (Relyea 2000). Because this study was conducted in a controlled laboratory environment, and specimens were housed at equal densities and fed *ad libitum*, it is unlikely that the observed differences in denticle length were the result of competition. Instead, plasticity was probably induced by variation in feeding behavior.

Plasticity in traits that are important in resource acquisition provides a means for organisms to adaptively respond to environmental uncertainty. Southern toads breed in a variety of habitats (Ashton and Ashton 1988), and consequently their offspring face a great deal of environmental uncertainty. Theory predicts that when selective pressures favor different phenotypes in different environments, adaptive plasticity will evolve (Via and Lande 1985, Moran 1992). The results of this study suggest that selection favored the maintenance of plasticity in denticle length in Southern toads as a means of equipping an individual with a morphology that compliments feeding behavior.

Linear Morphometrics

Specimens from the two diet treatments exhibited different scaling relationships in four of the twelve measurements evaluated in this study. Measurements predominantly scaled with isometry in specimens from the filtering treatment (all except BCL, and BCPQ), whereas there was an even mixture of isometry and negative allometry in specimens from the rasping treatment. Interestingly, both the distance between the lateral corners of the articular processes of the palatoquadrate (PAQO) and the distance between the lateral margins of the ceratohyal articular facets just behind the hyoquadrate process (CAW) scaled with isometry in specimens from the filtering treatment and negative allometry in specimens from the rasping treatment. These measurements were also significantly greater than those of specimens from the rasping treatment. Because CAW is an estimate of the maximum width of the buccal cavity (Wassersug and Hoff 1979) and PAQO is essentially a measure of anterior buccal width, these differences suggest that specimens from the filtering treatment had wider buccal cavities likely capable of holding greater volumes. From a functional perspective, a larger buccal

volume translates to greater negative pressure within the buccal cavity when the buccal floor is elevated (just prior to inspiration). When the buccal floor is lowered at the beginning of inspiration, the greater negative pressure within the buccal cavity will presumably bring in a larger amount of fluid. Thus, it seems as though *B. terrestris* larvae responded to the filtering diet by developing and maintaining a larger buccal cavity that likely enhanced their ability to filter larger volumes of suspended food.

Despite differences across treatments, the results from the scaling analysis do generally agree with allometries predicted to characterize cranial development in tetrapods. For example, Emerson and Bramble (1993) predict that trophic structures in the facial region should scale with isometry or positive allometry whereas the sensory capsules and braincase should scale with negative allometry. In the present study, all of the trophic structures evaluated (those anterior to BCPQ) scaled with isometry with the exception of PAQO in the rasping treatment. Likewise, braincase length (BCL) scaled with negative allometry for both treatments, while otic capsule length (OCL) scaled with negative allometry in the rasping treatment and isometry in the filtering treatment.

Although THW, PAQL, SRA, EPW, and MPW scaled with isometry in specimens from both treatments, these measurements were significantly greater in specimens from the rasping treatment (Table 5). This suggests that these chondrocranial elements are functionally important in rasping feeding. The suprarostral cartilages (Fig. 8) are attached to the trabecular horns and function as the movable upper jaw in tadpoles (Cannatella 1999) and therefore are extensively involved in rasping food attached to substrate. The functional importance of the suprarostral cartilages in rasping feeding may explain the greater values in THW, EPW, and SRA observed in specimens from the

rasping treatment. Greater trabecular horn widths (THW) translate to a more robust structural component for attachment of the suprarostral cartilages (Fig. 8). Moreover, the trabecular horns extend forward from the ethmoid (Cannatella 1999), thus, a wider EPW (a measure of the minimum width of the ethmoid plate posterior to the confluence of the trabecular horns) may also be the result of the need to strengthen the support of the trabecular horns. Although width of the suprarostral cartilages was not directly measured in this study, it is likely that these cartilages were wider in specimens from the rasping treatment because they possessed significantly wider SRAs (distance between the atriculations of the suprarostral cartilages to the trabecular horns). If this were true, then specimens from the rasping treatment not only had wider denticle rows, but wider suprarostral cartilages as well, both of which provide a larger surface area for rasping food from substrates.

The difference across treatments in PAQL (length of the articular process of the palatoquadrate) is interesting because this portion of the palatoquadrate serves as an attachment site for the three primary jaw depressor muscles (hyoangularis, quadratoangularis, and suspensorioangularis; Fig. 8) (Cannatella 1999). As these muscles contract they create tension in the mandibulo-suprarostral ligament (Fig. 8), which causes the upper jaw to open (Cannatella 1999). It may be that rasping feeding requires larger jaw depressor muscles than filtering suspension, and for that reason, specimens from the rasping treatment exhibited greater PAQLs. However, because detailed information on the importance of the jaw depressor muscles in filtering and rasping feeding is lacking, drawing anything more than tentative conclusions is difficult.

The muscular process of the palatoquadrate serves as the attachment site for the orbitohyoideus and suspensoriohyoideus muscles (Fig. 8). The primary function of the orbitohyoideus is buccal depression; however, Gradwell (1972) hypothesized that buccal depression may be an entirely passive process during normal gill irrigation, because of elastic recoil of the orbitohyoideus. This hypothesis was supported by electromyographic data from Larson and Reilly (2003) that indicated that in *Rana catesbiana* the orbitohyoideus was always active during rasping feeding and was either entirely inactive, or produced only low amplitude bursts of activity, during normal gill irrigation. In the present study, the differences observed in MPW (muscular process of the palatoquadrate width) are likely due to disparities in the size of the orbitohyoideus. Specimens from the rasping treatment used this muscle more often than those from the filtering treatment, and as a consequence they developed larger musculature, which then requires a larger attachment site. Moreover, the significantly greater MPW in specimens from the rasping treatment also suggests that the orbitohyoideus may play a lesser role in filtering suspension. Instead, it may be that the best way to enhance suspension feeding is by simply increasing buccal volume. Indeed, comparative studies suggest that species of microphagous suspension feeding tadpoles typically have greater buccal volumes than generalized species of tadpoles (Wassersug and Hoff 1979, Felsenstein 1985).

Geometric Morphometrics

Canonical variates analysis indicated that specimens from the two diet treatments were significantly different in terms of their chondrocranial morphology for both the whole ontogeny and terminal shape datasets. Moreover, results from the terminal shape CVA suggest that prolonged exposure to a particular diet treatment exacerbated the

effects of that treatment on morphology. Larson (2004) was the first to provide evidence of intraspecific variation in chondrocranial shape of *Bufo americanus* tadpoles. While Larson's (2004) study documented considerable variation in chondrocranial shape, the specimens used in analysis were from three different localities, and presumably three different clutches. The specimens used in the present study were all from the same egg clutch therefore it is unlikely that the observed differences in shape were due to genetic variation or maternal effects. Instead, the results of this study indicate that variation in feeding behavior can promote a surprising degree of shape differences, even among siblings.

A multitude of biological factors have been shown to influence external morphology (Smith and Van Buskirk 1995; Relyea 2001; Relyea 2003), and to a lesser extent internal morphology (but see: Relyea and Auld 2004; Castaneda et al. 2006). Yet, prior to this study, none quantified the effects of diet and feeding behavior on the morphology of the chondrocranium. Future investigations are needed to identify other potential causes, and the prevalence of intraspecific variation in chondrocranial morphology. Based on the results of this study, future work is needed to generate a better understanding of what, and how, ecological factors influence food selection. Many factors (e.g. light intensity, predator presence, nutrient availability, etc.) could either directly or indirectly influence food selection and/or food availability leading to subsequent variation in chondrocranial shape. Finally, the consequences larval morphological variation has on the adult stage would potentially provide a better understanding of the sources of variation in adult populations.

Table 1. Descriptions of linear measurements of the chondrocranium (modified from Larson 2004)

Measurement	Description
PAQL	The length of the articular processes of the palatoquadrate
THL	Distance from the confluence of the trabecular horns to the level of their anterior margin
SRA	Distance between the articulations of the suprarostral cartilages to the trabecular horns (a measure of gape width)
PAQO	Distance between lateral corners of the articular processes of the palatoquadrate cartilages
THW	Proximal trabecular horn width
EPW	Minimum width of the ethmoid plate posterior to the confluence of the trabecular horns
MPW	Width of the muscular process of the palatoquadrate
CAW	Distance between the lateral margins of the ceratohyal articular facets just behind the hyoquadrate process
BCPQ	Distance between the braincase and the most lateral margin of the subocular bar of the palatoquadrate
MW	Distance between the most lateral points of the ocular bar (maximum width)
OCL	Maximum length of the otic capsule
BCL	Length of the braincase from the posterior margin of the otic capsules to the confluence of the trabecular horns.

Table 2. Description of landmarks used in geometric morphometric analysis.

Landmark	Description
1	Anterolateral corner of the trabecular horn
2	Anteromedial corner of the trabecular horn
3	Anterolateral corner of the articular process of the palatoquadrate
4	Anteroventral margin of the muscular process of the palatoquadrate
5	Posterteroventral margin of the muscular process of the palatoquadrate
6	Posterior confluence of the hyoquadrate process with the palatoquadrate
7	Lateral margin of the ascending process
8	Medial margin of the ascending process
9	Maximum anterior curvature of the otic capsule
10	Maximum posterior curvature of the otic capsule
11	Confluence of the trabecular horns

Table 3. Filtering Treatment: Results of reduced major axes regressions of linear measurements of the chondrocrania against SVL. Confidence limits that overlap the value $k = 1$ indicate isometry, whereas confidence limits that fall below or above a value of $k = 1$ indicate negative and positive allometry, respectively.

Measurement	Intercept	Slope	R2	95% LCL	95% UCL	Scaling
PAQL	-1.13	0.975	0.696	0.8412	1.11	Isometry
THL	-0.9452	0.8917	0.3954	0.718	1.065	Isometry
SRA	-0.8326	0.8769	0.6285	0.7433	1.011	Isometry
PAQO	-0.5676	1.046	0.8045	0.9307	1.162	Isometry
THW	-1.741	1.247	0.7389	0.9735	1.407	Isometry
EPW	-1.422	1.202	0.8053	0.9662	1.335	Isometry
MPW	-0.999	0.9196	0.6844	0.7905	1.049	Isometry
CAW	-0.3221	0.8956	0.7708	0.7884	1.003	Isometry
BCPQ	-0.6809	0.8526	0.8157	0.7611	0.9442	Negative Allometry
MW	-0.2811	0.924	0.8001	0.8207	1.027	Isometry
OCL	-0.6606	0.8034	0.8205	0.7183	0.8885	Negative Allometry
BCL	-0.4067	0.9643	0.8433	0.8688	1.06	Isometry

Table 4. Rasping Treatment: Results of reduced major axes regressions of linear measurements of the chondrocrania against SVL. Confidence limits that overlap the value $k = 1$ indicate isometry, whereas confidence limits that fall below or above a value of $k = 1$ indicate negative and positive allometry, respectively.

Measurement	Intercept	Slope	R2	95% LCL	95% UCL	Scaling
PAQL	-1.053	0.9539	0.5691	0.7973	1.11	Isometry
THL	-0.8804	0.83	0.3643	0.6645	1.005	Isometry
SRA	-0.8971	0.9746	0.6305	0.8265	1.123	Isometry
PAQO	-0.3502	0.8077	0.72	0.7009	0.9146	Negative Allometry
THW	-1.455	1.02	0.6589	0.8708	1.169	Isometry
EPW	-1.201	1.018	0.6804	0.8737	1.161	Isometry
MPW	-1.047	1.023	0.4779	0.838	1.208	Isometry
CAW	-0.2851	0.8702	0.7571	0.763	0.9774	Negative Allometry
BCPQ	-0.7067	0.8808	0.7629	0.7736	0.9881	Negative Allometry
MW	-0.2013	0.8579	0.8004	0.7621	0.9538	Negative Allometry
OCL	-0.5752	0.7284	0.7272	0.6333	0.8236	Negative Allometry
BCL	-0.3166	0.8896	0.8168	0.7944	0.9848	Negative Allometry

Table 5. Results of one-way ANOVAs (measurement x treatment) on linear measurements of the chondrocrania functionally important in feeding. Linear measurements for each specimen were regressed against the corresponding SVL to remove the influence of size, the residuals from the regressions were then collected and used in statistical analysis

Measurement	$\mathbf{F_{1, 130}}$	***p*-value**	**Tukey-Kramer *(post hoc)***
THL	0.1131	0.7372	NS
PAQO	15.38	0.0001	Filtering > Rasping
THW	17.82	< 0.0001	Rasping > Filtering
PAQL	25.85	< 0.0001	Rasping > Filtering
SRA	10.13	0.0018	Rasping > Filtering
EPW	6.99	0.0092	Rasping > Filtering
MPW	22.14	< 0.0001	Rasping > Filtering
CAW	19.63	< 0.0001	Filtering > Rasping

Figure 1: Measurements taken from lateral photographs of specimens (A), snout-vent length (SVL). Distance measured to obtain the length of the longest denticle row (DL) for each specimen (B).

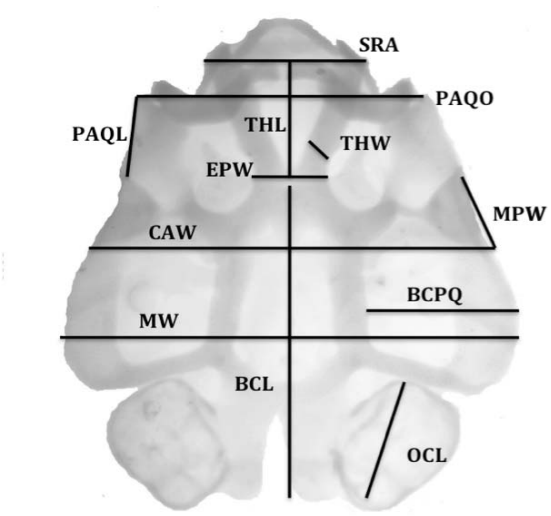

Figure 2. Linear measurements of the chondrocranium superimposed on a specimen from the rasping diet treatment (Gosner 34, SVL: 11.22mm). Descriptions of the measurements are provided in Table 1.

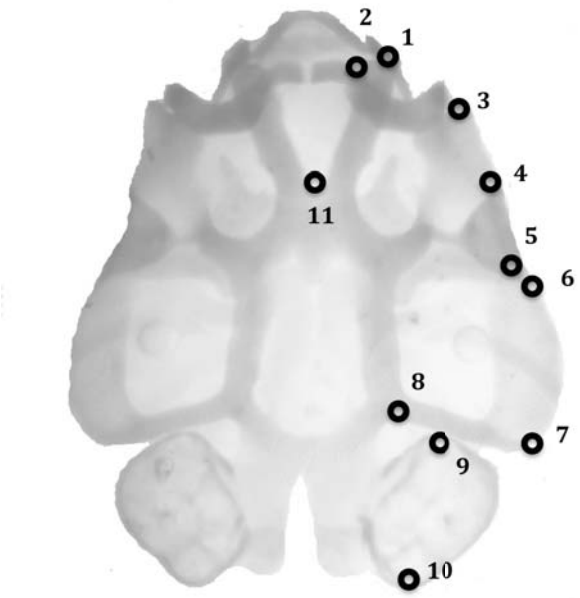

Figure 3. Landmarks used for geometric morphometric analysis superimposed on a specimen from the rasping diet treatment (Gosner 34, SVL: 11.22mm). Landmark locations are described in Table 2.

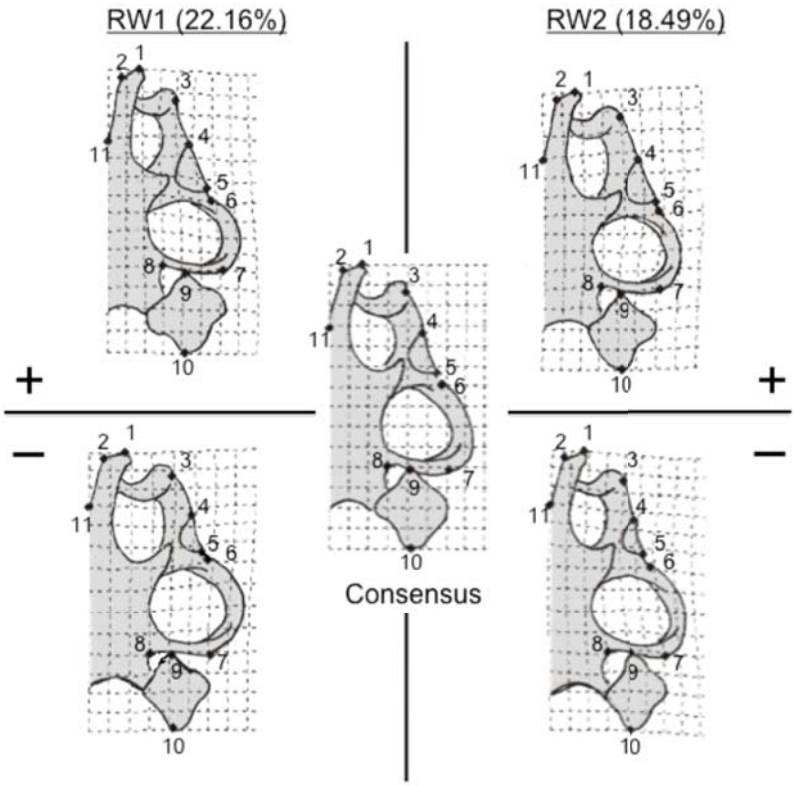

Figure 4. Whole Ontogeny Analysis. Thin-plate spline deformation grids depicting chondrocranial shape change (relative to consensus form) at positive and negative extremes along the first two relative warp axes. At the center is the consensus form, the left side shows positive (above) and negative extremes along the first RW axis, and the right side shows positive and negative extremes along the second RW axis. Outlines are only meant to facilitate visualization of shape change, and do not represent a particular specimen.

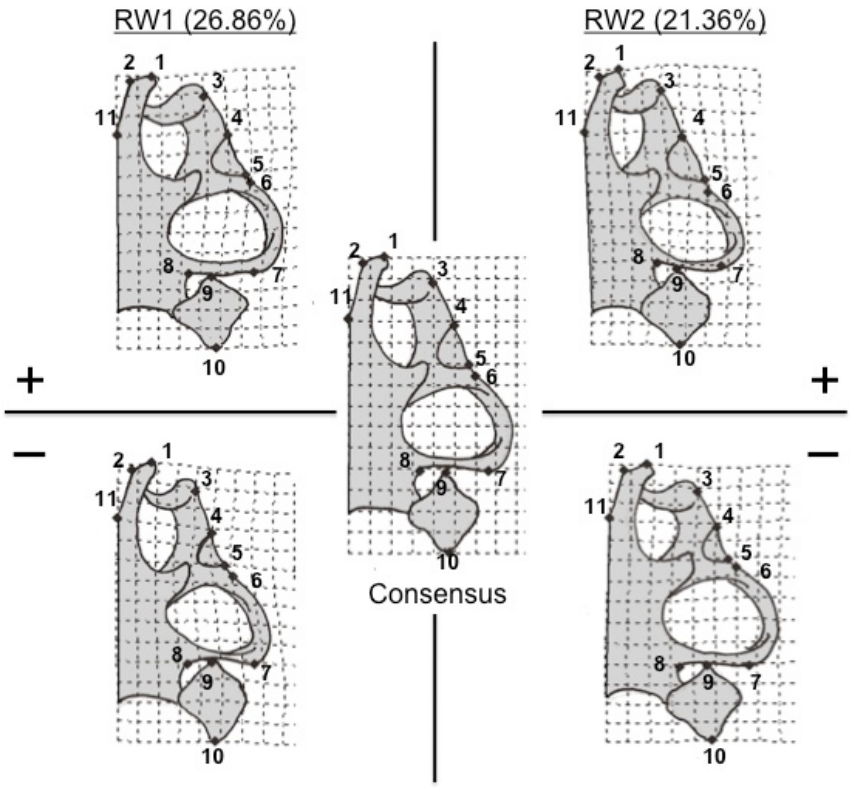

Figure 5. Terminal Shape Analysis. Thin-plate spline deformation grids depicting chondrocranial shape change (relative to consensus form) at positive and negative extremes along the first two relative warp axes. At the center is the consensus form, the left side shows positive (above) and negative extremes along the first RW axis, and the right side shows positive and negative extremes along the second RW axis. Outlines are only meant to facilitate visualization of shape change, and do not represent a particular specimen.

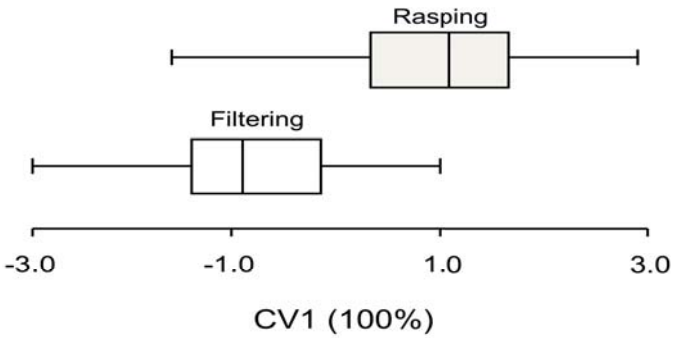

Figure 6. Box plot of specimens CV1 scores, the horizontal lines on the ends of the boxes indicate the range of scores, and the vertical line inside each box represents the mean for that treatment. Treatment groups are separated on the y-axis to enhance visual interpretation.

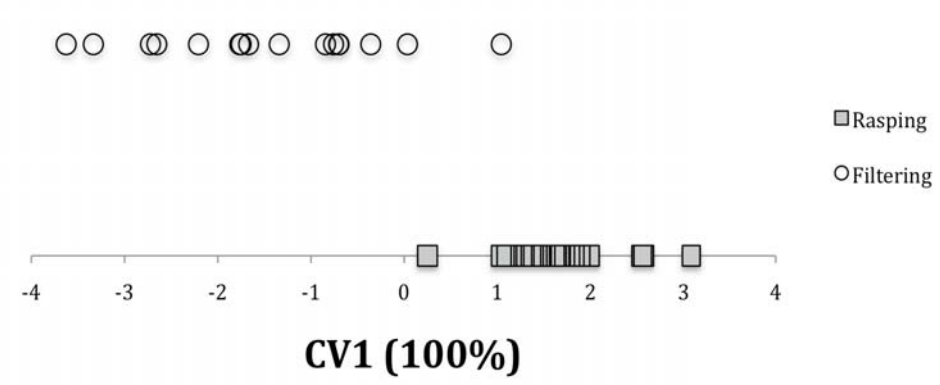

Figure 7. Scatterplot showing the scores of terminal shape specimens on the first CV axis. Treatment groups are separated on the y-axis to enhance visual interpretation.

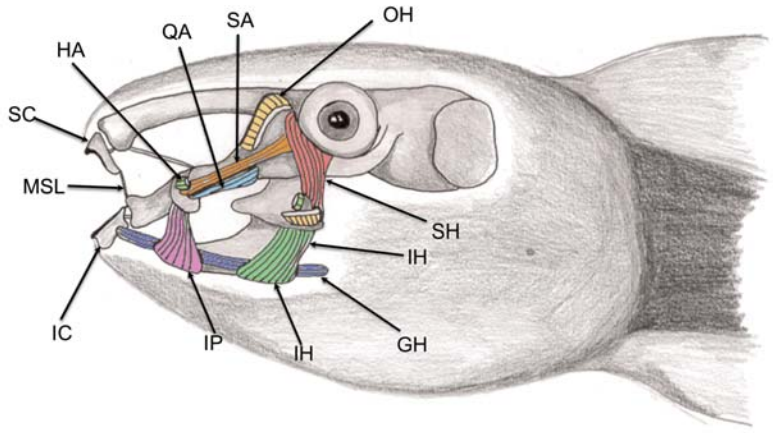

Figure 8. Lateral view of the larval anuran chondrocranium showing the location of the suprarostral cartilages (SC), infrarostral cartilages (IC), orbitohyoideus (OH), suspensoriohyoideus (SH), quadratoangularis (QA), suspensorioangularis (SA), hyoangularis (HA) geniohyoideus (GH), mandibulo-suprarostral ligament (MSL), interhyoideus (IH), and intermandibularis posterior (IP). In this illustration the suspensoriohyoideus, quadratoangularis, hyoangularis, and geniohyoideus are all contracted, as they would be when the mouth is open. Redrawn from Gradwell 1972.

Chapter 2

The effects of light intensity on morphology and development of larval Southern toads (*Bufo terrestris*)

Introduction

Canopy closure over aquatic habitats has been identified as an environmental variable that can impact not only development of larval anurans, but also their species distribution and overall performance (Werner and Glennemeier 1999; Schiesari 2006; Thurgate and Pechmann 2007). Canopy closure limits light penetration, which subsequently affects temperature and the composition and productivity of the photosynthetic organisms present in aquatic environments (Werner and Glennemeier 1999; Schiesari 2006). Because larval anurans are ectothermic and predominantly herbivorous (McDiarmid and Altig 1999), canopy closure has the potential to profoundly, albeit indirectly, influence their growth and development. In general, larval anuran growth is a function of diet quality and quantity, whereas time to metamorphosis is a function of environmental temperature (Marian and Pandian 1985). Lower temperatures typically suppress development more than growth (Smith-Gil and Berven 1979), and larval anurans reared in colder temperatures typically metamorphose later, yet at larger sizes, than conspecifics reared in warmer temperatures (Alvarez and Nicieza 2002). Closed canopy aquatic environments prolong development (Werner and Glennemeier 1999; Schiesari 2006; Thurgate and Pechman 2007), however, individuals reared in these environments typically do not attain larger sizes due to the lack of quality food resources (Werner and Glennemeier 1999; Schiesari 2006; Thurgate and Pechman 2007).

Open-canopied aquatic environments typically experience higher levels of primary production, whereas closed-canopied ponds provide mainly detritus based resources (Werner and Glennemeier 1999). This resource dichotomy may be responsible for variation in not only growth, but also in feeding behavior. For example, many species of larval anurans are known to use filtering and/or rasping feeding behaviors in order to consume either planktonic material from the water column or organic material from sediments and submerged substrates (Hoff et al. 1999). Organic material suspended in the water column is consumed by filtering, whereas consuming organic material attached to a substrate requires rasping with the keratinized beak and labial teeth which creates a suspension that may be subsequently filtered (Hoff et al. 1999). In a closed-canopied environment, where concentrations of phytoplankton are reduced, larval anurans may be restricted to feeding almost exclusively by rasping detritus or other benthic substrates. Alternatively, in open-canopied ponds where there is a greater diversity of food resources (Schiesari 2006) larval anurans likely feed by filtering suspended phytoplankton as well as rasping organic material from substrates.

Because the muscular mechanics associated with rasping feeding and suspension feeding differ (Larson and Reilly 2003), these feeding behaviors may produce disparities in jaw musculature (Bernays 1986; Wainwright et al. 1991; Thompson 1992). Changes in musculature may have subsequent effects on the size and/or shape of the surfaces upon which those muscles attach (Bernays 1986). This may be especially true for the cartilaginous larval anuran chondrocranium because the resultant forces of muscular contractions have been shown to influence the shape of primary cartilage (Herring 1993). Finally, lower temperatures in closed canopy environments may exacerbate the effect of

feeding musculature on chondrocranial morphology. Because development is prolonged in these conditions, the factors influencing shape occur over a greater temporal scale.

Only recently have studies begun to evaluate the influence of environmental factors on chondrocranial morphology. Results of previous studies indicate that both temperature regime (Jorgensen and Sheil 2008) and diet composition (Chapter 1) are capable of generating significant intraspecific variation in chondrocranial shape. However, the potential for diet composition and/or temperature to generate chondrocranial shape variation outside of controlled laboratory settings has yet to be evaluated. Given what is known regarding environmental influence on chondrocranial shape, it seems likely that canopy closure is capable of producing the disparities in aquatic environments necessary to generate significant morphological variation in the larval anuran chondrocranium.

In addition to differences in chondrocranial shape, canopy closure may also elicit a plastic response in specific variables such as denticle length. Studies have documented denticle length plasticity in several species of larval anurans (*Rana pipiens* and *Rana sylvatica* Relyea 2000; Relyea and Auld 2005; *Bufo terrestris* Chapter 1). Larval Southern toads (*Bufo terrestris*) that feed only by rasping substrates grow significantly longer denticles than siblings that are fed suspended particles (Chapter 1). Canopy closure may elicit a similar response, whereby individuals reared in closed canopy environments with little phytoplankton feed primarily by rasping and as a result develop larger denticles than conspecifics raised in open canopy environments.

The goal of this study was to determine the effects of a simulated canopy-closure gradient on chondrocranial morphology and denticle length of larval Southern toads

(*Bufo terrestris*). Developmental times and measurements of snout-vent length (SVL) were also compared across treatments. Several methods were used to evaluate chondrocranial morphology across shade treatments: (1) scaling relationships of the chondrocranial cartilages were quantified to describe the growth of specific chondrocranial elements in relation to overall size, and (2) geometric morphometrics were used to analyze fine-scale variation in chondrocranial shape among treatments. Geometric morphometric data were obtained from specimens representing multiple ontogenetic stages. Chondrocranial shape was evaluated throughout ontogeny and at late developmental stages to provide information on the trajectories at which changes in shape proceed. This methodology allows one to determine if shape variation among treatments is distinguishable throughout ontogeny, or if morphologies gradually diverge so that clear differences are only present late in ontogeny.

Methods and Materials

Focal Species

Southern toad (*Bufo terrestris*) tadpoles were used as the focal organism for this study. Because this species is reportedly indiscriminate when selecting egg deposition sites (Gibbons and Semlitsch 1991), larvae can potentially encounter a wide variety of environmental conditions (canopy closure, resource quantity and quality, etc.). Larvae typically reach metamorphosis 30-55 days after hatching (Ashton and Ashton 1988).

Mesocosms

Opaque plastic wading pools (n = 12, diameter = 1.67m, depth = 20.5 cm) were used to rear tadpoles (Figure 9). Each pool, or mesocosm, was separated into four quadrants by fiberglass window screening so that 100 *B. terrestris* siblings could be

housed in each quadrant. Pools were assigned to one of three shade treatments (0% shade, 30% shade, and 70% shade, n=4). There was no screen covering placed over 0% shade pools, 30% shade cloth screening (U.S. Nettings©) and 70% shade cloth was used for the remaining treatments. Thurgate and Pechmann (2007) showed that a 70% reduction in light intensity for experimental purposes is ecologically relevant, when they measured photosynthetically active radiation (PAR) at an open and closed-canopy pond.

Pools were arranged in a set of four blocks (one block consisted of one 0%, 30%, and 70% shade treatment), which were separated by approximately 10 meters. All pools were located in an open-canopied field and did not receive additional shade from nearby trees or vegetation.

Fifteen grams of dried leaf litter (primarily *Quercus spp*.) was applied to each quadrant, and the mesocosms were then filled with water from a nearby pond (approx. 30 gal.), where *B. terrestris* larvae and breeding adults have been observed (pers. obsv.). After filling, all mesocosms were left undisturbed from 20 May 2007 until 14 June 2007, to allow for the development of algal communities representative of the respective shade treatments. Once algal communities were established, 100 *B. terrestris* eggs were placed in each quadrants of each pool. Eggs used in this study were taken from one of four clutches collected in Bulloch County, GA. Each pool received a total of 400 eggs consisting of 100 eggs from each of the four clutches. Eggs were placed in pools so that each quadrant would house 100 full siblings and each pool would house 400 tadpoles from four different egg clutches.

Temperature

Data loggers were placed in each pool to record hourly temperature throughout the duration of the experiment. Temperature data from three (two 0% shade pools, and one 70% shade pool) pools were lost due to failure of the data loggers in those pools. However, water temperatures for each pool was recorded on six different occasions using a handheld thermometer, and in each case the difference in temperatures within treatment groups never exceeded 0.2 °C. This suggests that the temperature regimes experienced by pools for which a complete temperature dataset is lacking, were likely similar to those recorded for other pools from the same treatment. Preliminary analysis of hourly temperature revealed that temperatures in pools from the three shade treatments were the same between the hours of 7pm and 1pm of the following day (Kruskal-Wallis: X^2 = 0.54, df = 2, p = 0.68; 0%: 24.07 °C ± 0.10; 30%: 24.02 °C ± 0.09; 70%: 24.29 °C ± 0.09). Therefore, only temperatures between the hours of 1pm-7pm were used to compare mean temperatures among treatments because pool temperatures were different during this time frame. Finally, because within treatment temperature variation was minimal, the temperatures between the hours of 1pm-7pm for all pools within a single treatment were averaged to produce a grand treatment mean to describe the daytime variation among light intensity treatments.

Primary Productivity

Phytoplankton and periphyton communities were sampled every two weeks for the duration of the experiment (6 Jun., 11 Jul., 24 Jul., 9 Aug., 29 Aug., 14 Sept., 24 Sept. and 12 Oct.). Measurements of chlorophyll-a were used to quantify phytoplankton and periphyton biomass within pools. After evaluating data from an array of various aquatic

environments, Morin et al. (1999) suggested a strong log-linear relationship between chlorophyll-a and primary productivity. Therefore using chlorophyll a as a course proxy for primary productivity is acceptable (Morin et al. 1999; Death and Zimmerman 2005). To determine phytoplankton concentrations, 100-ml samples of subsurface water (e.g. 6 cm. below the surface) from each pool were filtered through a Whatman GF/F glass fiber filter. The filters were then stored in a dark freezer until chlorophyll-a extraction was conducted. For chlorophyll-a extraction, the filters were placed in 8ml of 90% acetone for 24 hours at -20°C. A Turner Designs 700 fluorometer was used to determine chlorophyll-a concentrations of the sample following EPA method 404 outlined by Arar and Collins (1997).

Ceramic tiles (10.16 cm x 10.16 cm) were placed in each pool at the beginning of the experiment to serve as a standard substrate to measure the growth of periphyton. On sampling dates the tiles were gathered and returned to the lab, where they were scraped with a razorblade, rinsed, and the resulting suspension was filtered through a Whatman GF/F glass fiber filter. Filters were stored in the dark at -20°C until analysis. Filters were ground with a mortal and pestle for three minutes in 90% acetone and refrigerated for 18 hours. Chlorophyll-a concentrations were then determined using a T.D. 700 fluorometer following Arar and Collins (1997).

Monitoring Specimens & External Morphology

Throughout the experiment, tadpoles in the pools were monitored three or more times per week. Tadpoles were periodically removed and euthanized in chlorotone. Tadpoles were selected such that multiple specimens from each treatment were selected over a range of developmental stages (Gosner; 28-38). Following euthanization, each

specimen was staged and its mass (after blotting with a paper towel) was recorded. Specimens were stored in 10% buffered formalin until morphological measurements were taken. Specimens were photographed in a lateral view, and snout-vent length (SVL) was measured using TpsDig v. 1.18 (Rohlf, 1998, Department of Ecology and Evolution, SUNY, Stony Brook). The length of the longest denticle row (hereafter termed denticle length) was measured using a dissecting scope fitted with an ocular micrometer.

Chondrocranial Morphology

To visualize chondrocranial morphology, all specimens were enzyme cleared and stained for both cartilage and bone following the procedures described by Dingerkus and Uhler (1977). Dorsal views of the chondrocrania of all specimens were photographed with a digital camera. Photographs were digitized and 12 linear measurements from each specimen were obtained using TpsDig v. 1.18 (Rohlf, 1998, Department of Ecology and Evolution, SUNY, Stony Brook). The measurements describe the general shape of the chondrocranium (e.g., braincase length), and the shape of functionally important structures (e.g., muscular insertion sites such as the palatoquadrate and muscular process; see Larson 2002; 2004; 2005). Eleven landmarks were used for geometric morphometric comparisons of chondrocranial shape (Figure 3, Table 2 in Chapter 1). Landmarks were chosen based on their ability to represent the entirety of geometric form, and to describe functionally important structures (Larson 2002, 2004, 2005; Figure 3, Table 2 in Chapter 1).

Analysis

All morphological data was log10 transformed to achieve a normal distribution: nonparametric tests were used for variables that were not normally distributed following

transformation. To determine the effect of treatment on body size (SVL), specimens were grouped into early (Gosner 28-31), middle (Gosner 32-35), and late (Gosner 36-38) developmental stage categories. Preliminary analysis indicated that random variation attributable to replicate pools within a single shade treatment was not evident (Table 6); therefore, data for all specimens within each treatment were pooled for analysis. Specimens were grouped by treatment and one-way ANOVAs (treatment x log10 SVL) were used to determine if early, middle, and late stage specimens differed in size across treatments.

In order to test the effect of treatment on denticle length, denticle length was regressed against SVL and the residuals were collected to remove the influence of body size variation in denticle length. Residual denticle length was analyzed using analysis of variance (ANOVA).

Reduced major axes regressions of each of the 12 $\log_{10}$-transformed chondrocranial measurements on $\log_{10}$ SVL were used to obtain regression slopes describing the scaling relationships of the linear measurements. To test the null hypothesis of isometric scaling, 95% confidence intervals were calculated for the reduced major axes regression slopes (Bohonak, A. J. and K. van der Linde. 2004. RMA: Software for Reduced Major Axis regression for Java). Here a value of $k = 1$ indicates isometric scaling. Thus, if the confidence intervals fail to overlap a value of 1, the null hypothesis of isometry is rejected, confidence intervals greater than or less than 1 indicate positive allometry (CI >1) and negative allometry (CI <1).

Landmark data for all specimens were analyzed using two approaches. First, relative warps analysis (RWA) was used to quantify variation in the landmark data.

Relative warp analysis generates partial warp scores (n =16 for this study; number of partial warps= 2p- 6; where p is the number of landmarks) and two uniform components. Thin-plate spline deformation grids depicting chondrocranial shape change at both positive and negative extremes along the first two relative warp axes were obtained to enhance visual interpretation of morphological data. Finally, the partial warp scores and uniform components were subjected to canonical variates analysis to determine if specimens could be correctly classified to their respective diet treatments based on chondrocranial shape. This analysis was conducted on specimens from a range of ontogentic stages (Gosner 28-38), and a group of prometamorphic (Etkin 1968) specimens (Gosner 36-38). Analyzing both the entire ontogenetic series and late stage prometamorphic specimens was done to determine if the effects of the shade treatments are discernable in all specimens regardless of developmental stage, or if the treatment effects accumulate slowly and are only visible at the later developmental stages.

Given that shade affects both temperature and primary productivity (Werner and Glennemeier 1999, Schiesari 2006), quantifying the amount of morphological variation solely attributable to either temperature or primary productivity is difficult. For example, if statistical analysis were to reveal that phytoplankton biomass in a treatment had a significant effect on a particular morphological variable, one would not necessarily be able to accurately identify which environmental factor was responsible for the observed effect on morphology. Instead the effect may be due to the treatment, because the treatment (shade) is presumably affecting phytoplankton populations. For this reason temperature and primary productivity data are presented in a descriptive manner and are provided to show their relationship to a particular variable of interest for comparative

purposes. Thus, while interpretations of the effects of temperature and primary productivity on morphology are not supported by statistical analysis; they are discussed in a manner that is congruent with what is known regarding the effects of temperature and diet composition on larval anurans.

Results

SVL, Developmental Time, Temperature

There was no difference in SVL among treatments between early ($F_{2,103}$= 0.373; p= 0.689) and middle developmental stages ($F_{2,100}$= 0.679; p= 0.509) (Table 7). Late developmental stages were significantly different in SVL ($F_{2,56}$= 6.8045; p=0.002). Tukey-Kramer *post hoc* tests indicated that late stage specimens from the 0% light intensity treatment were smaller than specimens from the 30% and 70% light intensity treatments. There was no difference in SVL between 30% and 70% specimens.

Developmental time differed significantly across treatments (Kruskal-Wallis: early: H = 49.24, df = 2, p = < 0.0001; middle: H = 40.57, df = 2, p = < 0.0001; late: H = 25.32, df = 2, p = < 0.0001) and increased with increasing light intensity (Table 7, Fig. 10). The difference in developmental times from the 0% and 70% treatments was especially pronounced, as it took specimens from the 70% treatment more than twice as long as it took 0% specimens to reach early, middle, and late developmental stages (Table 7; Fig. 10). Daytime temperature (between 1pm and 7pm) differed significantly among treatments (H = 191.63, df = 2, p = < 0.0001). As expected, temperature decreased with increasing shade (Fig. 11), and higher temperatures were associated with more rapid development.

Primary Productivity

Between the first (20 June) and the second (11 July) sampling dates, chlorophyll a concentrations declined sharply in both the 0% and 30% shade treatments (Fig. 12). This initial decline was not observed in the 70% shade treatment. After the average date at which specimens from the 0% and 30 % shade treatments had reached late developmental stages, there was an increase in chlorophyll a concentrations of both phytoplankton and periphyton concentrations in the 0% shade pools. When considered with the initial declines prior to metamorphosis this suggests that phytoplankton and periphyton populations were grazed by tadpoles and then producer biomass began to recover as the tadpoles began to metamorphose.

Chlorophyll-a concentrations from the 70% treatment did not follow the patterns observed for the 0% and 30% shade treatments (Fig. 12). Periphyton concentrations were lower on the first sampling date than in the other treatments and declined only slightly between the first and second sampling dates. Additionally, periphyton concentrations remained relatively low throughout the duration of the experiment in the 70% shade pools. Phytoplankton concentrations were also lower than other treatments on the first sampling date, and unlike the others, they increased between the first and second sampling dates. The absence of a sharp decline in either phytoplankton or periphyton concentrations between the first two sampling dates (as in the 0% and 30% light intensity treatments) in the 70% treatment may be indicative of the effects of temperature on development and/or activity levels.

Denticle Length

There was a significant effect of shade treatment on size adjusted denticle length (ANOVA: $F_{2,261}$= 21.77; p= <0.0001). *Post hoc* analysis revealed no difference in denticle length between 30% and 70% treatments. However, specimens from 30% and 70% treatment had greater denticle lengths than 0% specimens.

Linear Morphometrics

The measurements used in this analysis scaled primarily with negative allometry in all treatments (Table 8). Specimens from the 0% shade treatment scaled with negative allometry in every measurement except trabecular horn width (THW), which scaled with isometry (Table 8). Specimens from the 30% and 70% shade treatments exhibited isometric scaling in ethmoid process width (EPW) (Table 8). Muscular process width of the palatoquadrate (MPW) scaled with positive allometry in 30% specimens and isometry in 70% specimens, and 70% specimens scaled with isometry in length of the articular processes of the palatoquadrate (PAQL) and the distance between the articulations of the suprarostral cartilages to the trabecular horns (SRA) (Table 8).

Geometric Morphometrics: Whole Ontogeny

Thin-plate spline deformation grids depicting chondrocranial shape change (relative to the consensus form) at positive and negative extremes along the first two relative warp axes are presented in Figure 13. Together the first two RW axes explained 38% of the variation present in the dataset. The first relative warps axis (RW1) explains variation among landmarks 1 through 8 (Fig. 13). When compared to the consensus form, the positive extreme of axis one (RW1+) depicts landmarks 3 and 4 as lateral to their positioning on the consensus form. Landmarks 5 and 6 are displaced posteriorly

and medially, landmark 7 posteriorly, and 8 medially. Landmarks 1 and 2 is slightly lateral to the consensus form, and the interlandmark distance between 4 and 5 is greater than the distance shown in the consensus form. Finally, the spatial configuration of landmarks 5, 6, 7, and 8 shows that at the positive extreme these landmarks are much closer in relation to each other than they are in the consensus form. Therefore specimens scoring on the positive end of RW1 appear to be wider at the anterior portions of the chondrocranium, possess an enlarged muscular process of the palatoquadrate (distance between 4 and 5), and have a compressed orbit. The negative extreme of each relative warp axis shows the opposite pattern of the positive extreme.

The positive extreme of the second relative warps axis (RW2+) shows landmark 1 to be slightly lateral to the consensus form, and landmarks 5 and 6 appear anterior to their consensus location. Landmarks 4 and 7 are posterior to their consensus locations. These spatial configurations result in an increase in the distance between landmarks 3 and 4, and a pronounced decrease in the distance between landmarks 4 and 5. Thus, specimens that scored high on the second relative warp axis are characterized by possessing a reduced muscular process width of the palatoquadrate, and an exaggerated length of the articular process of the palatoquadrate. In contrast, specimens that scored low on the second relative warp axis have an enlarged muscular process width of the palatoquadrate, and a reduced length of the articular process of the palatoquadrate.

Results of the CVA indicate significant differences in chondrocranial shape across treatments (Wilks'- Lambda: $F_{18,113} = 4.78$, $p = < 0.0001$). Of the 264 specimens, 82% (n = 216) were correctly classified to their respective shade treatment based on chondrocranial shape. Specimens from the 70% shade treatment scored higher on the first

CV axis than those from the 0% and 30% shade treatment (Fig. 15). Specimens from the 30% and 70% shade treatments scored slightly higher on the second CV axis; however, there was a considerable amount of overlap, and the treatment groups were not clearly distinguished by separation along the second CV axis (Fig. 15).

Geometric Morphometrics: Terminal Shape

The first six relative warps explained 76% of the variation present. Thin-plate spline deformation grids depicting chondrocranial shape change (relative to the consensus form) are presented in Figure 14. Together the first two axes explained 43% of the variation present in the dataset. At the positive extreme of the first relative warp axis (RW1+), landmarks 1, 4, and 7, all are located laterally to their locations on the consensus form. Landmarks 5, 6, and 8, are located posterolateral to their spatial configurations on the consensus form, and landmark 3 is medial to its consensus configuration. The posterior location of landmark 5 results in an increased distance between landmarks 4 and 5, therefore muscular process width of the palatoquadrate was greater in specimens that scored high on RW1.

At the positive extreme of the second relative warp axis (RW2+) landmarks 1, 2, 8, and 9 all appear to be medial to their respective locations on the consensus form. Landmarks 5, 6, and 7 are shown as posterior to their respective locations on the consensus form. Once again, the posterior location of landmark 5 results in an increased distance between landmarks 4 and 5. This suggests that the muscular process width of the palatoquadrate was greater in specimens that scored high on RW2.

Results of the CVA indicate significant differences in late stage chondrocranial shape across treatments (Wilks'- Lambda: $F_{36,42} = 3.18$, $p = < 0.0002$). Forty-seven of 48

terminal shape specimens were correctly classified to their respective shade treatment based on chondrocranial shape data alone. The first CV axis separates 70% shade specimens from those raised in 30% and 0% shade (Fig. 16). The second CV axis separates specimens from the 0% and 30% shade treatments; specimens from the 0% shade treatment scored higher on the second CV axis than those from the 30% shade treatment (Fig. 8).

Discussion

The results of this study show that the shade treatments affected multiple features of larval *B. terrestris*. The shade treatments used in this study induced differences in SVL, developmental time, scaling patterns, denticle length, and chondrocranial morphology. These treatments also caused a significant reduction in temperature, which is one of the most influential environmental cues to young ectotherms (Hochachka and Somero 1984). Elevated temperatures typically stimulate rapid development with the cost of smaller size at metamorphosis in larval anurans (Smith-Gil and Berven 1979; Atkinson 1996; Merila et al. 2000; Alvarez and Nicieza 2002; Laugen et al. 2003). Thus, the rapid development and smaller sizes observed for specimens from the 0% shade treatment were likely due to temperature.

Because larger size at metamorphosis is correlated with increased fitness, fecundity, and shorter time to first reproduction in amphibian species (Semlitsch et al. 1988; Berven 1990), there is a trade-off between developing rapidly and escaping the dangers of many aquatic environments (i.e. predation, dessication, etc.) or postponing metamorphosis in order to attain greater size. For a species such as *B. terrestris* that breeds in both permanent (Ashton and Ashton 1988; Gibbons and Semlitsch 1991; pers.

obs.) and extremely ephemeral water bodies (Ashton and Ashton 1988; Gibbons and Semlitsch 1991; pers. obs.), minimizing time to metamorphosis in response to elevated temperatures is a valuable strategy. For example, as ponds dry, their surface area to volume ratio begins to increase, which subsequently causes temperature to rapidly increase (Merila et al. 2000). Responding to elevated temperatures by shortening time to metamorphosis provides larval anurans with a means to assess the risk of dessication and respond accordingly. Therefore, temperature is likely an honest indicator of pond drying. Alternatively, at lower temperatures, the risk of pond desiccation is not as great (or not perceived) and therefore development is delayed which in turn allows individuals to attain larger sizes at metamorphosis.

In addition to developmental time and size, shade treatment had a significant effect on denticle length. Specimens from the 0% shade treatment had significantly smaller denticles than those from the 30% and 70% shade treatments. Diet composition has been shown to elicit a plastic response in *B. terrestris* denticle length in a laboratory environment (Chapter 1). Individuals given a diet that required them to rasp substrates in order to obtain food developed larger denticles than siblings given a diet that was suspended in the water column, and did not require rasping behavior (Chapter 1). This suggests a relationship between shade treatment and diet composition/feeding behavior. It is possible that individuals from the 0% shade treatment spent a proportionally greater amount of time feeding by filtering suspension than their counterparts in the 30% and 70% shade treatments and therefore grew smaller denticles.

Since specimens from the 0% shade treatment developed the fastest, any effects of diet on denticle length would have the least amount of time to accrue. This does not

necessarily contradict the previous suggestion that a relationship between shade treatment and diet composition/feeding behavior produced the observed differences in denticle length. Instead, temperature and diet may affect denticle length morphology in a synergistic fashion. For example, if specimens from the 70% shade treatment feed primarily by rasping, then prolonged development means more rasping which likely results in greater denticle length.

In other species of larval anurans (*Rana pipiens* and *Rana sylvatica*) competition has been shown to induce denticle length plasticity (Relyea 2000; Relyea and Auld 2005). However, because of the design of this experiment it seems unlikely that there were any adverse effects of crowding and/or competition. Specimens were frequently and consistently removed from all pools throughout the experiment, thus alleviating crowding on a regular basis. Further, regardless of treatment, when the pools were visited tadpoles could easily be observed feeding throughout the pool and never at any point did they appear to be scrambling to consume a limited resource.

Further studies are needed to determine whether or not competition in the larval environment may induce denticle length plasticity in *B. terrestris*. Understanding how competition affects feeding behavior is also necessary, since feeding behavior has been shown to induce plasticity in denticle length in this species (Chapter 1).

Primary Productivity

Chlorophyll-a concentrations of both phytoplankton and periphyton samples declined sharply between the first two sampling dates in 0% and 30% shade pools. Since tadpoles have been shown to regulate primary productivity and alter phytoplankton and periphyton communities (Dickman 1968; Seale 1980; Seale and Beckvar 1980) the initial

reduction in biomass is likely to have been the result of grazing by the tadpoles in those pools. Additionally, after the average date at which specimens had reached later developmental stages (i.e. the time at which tadpoles were nearing metamorphosis and no longer feeding) chlorophyll-a concentrations began to increase almost immediately. This observation further suggests that the preliminary declines in phytoplankton and periphyton biomass is associated with grazing pressure from the tadpoles in those treatments.

In contrast to the 0% and 30% shade treatments, neither phytoplankton nor periphyton chlorophyll-a concentrations exhibited an initial decline in 70% pools. One possible explanation is that at the onset of the experiment these communities were grazed with less intensity than those in the 0% and 30% shade treatments. it is likely that the lower temperatures in the 70% treatment reduced grazing to some extent. Indeed, temperature is known to affect many behavioral and physiological variables that are ecologically relevant to ectotherms (Ultsch et al. in McDiarmid and Altig 1999), thus, lower temperatures in the 70% pools may have led to reduced activity levels and grazing.

Finally, it should be noted that periphyton communities may possess a significant proportion of heterotrophic components (Lock, et al. 1984). Although information on assimilation and nutritional value of the fungal, protozoan, and bacterial components potentially present within periphyton communities is mostly lacking, it is likely that these components are of some nutritional benefit to larval anurans (Altig et al. 2007). Thus, the periphyton chlorophyll-a concentrations used to describe this algal community potentially underestimate the quantity of available food resources in these samples. Future work

should quantify the role of the heterotropic algal components in larval anuran development.

Linear Morphometrics

The allometric scaling patterns of specimens were different in each of the three shade treatments. Interestingly, as light intensity decreased, measurements began to increasingly scale with isometry, and in one case positive allometry. The allometries observed thus far in larval anurans generally concur with allometric predictions for tetrapod cranial development (Larson 2004). Emerson and Bramble (1993) predict that trophic structures in the facial region should scale with isometry or positive allometry whereas the sensory capsules and braincase should scale with negative allometry. In the present study, measurements associated with the sensory capsules (OCL) and braincase (BCL) scaled with negative allometry in specimens regardless of light intensity treatment. However, measurements of trophic structures did not scale with either isometry or positive allometry in specimens from the 0% shade treatment.

The scaling patterns of specimens from the 0% shade treatment may once again be related to temperature. For example, elevated temperature may stimulate rapid development while retarding growth to such an extent that chondrocranial elements scale with negative allometry. Indeed, the fact that 0% shade specimens experienced the highest temperatures, fastest development, and were the smallest at late stages in development supports this hypothesis. In a study on the effects of temperature and temperature regime on chondrocranial shape, Jorgenson and Sheil (2008) demonstrated that both of the above factors affect the shape of the larval chondrocranium in *Anaxyrus americanus.* While diet may induce changes in chondrocranial allometry (Chapter 1), the

effects of temperature on growth and development may outweigh any effect of diet. Further studies are needed to isolate the relative contributions of temperature and diet to shape variation in the chondrocranium.

Larval *B. terrestris* given a rasping diet develop greater SRA, PAQL, THW, EPW, and MPW than siblings given a filtering diet (Chapter 1). Interestingly, all of these measurements scaled with isometry in specimens from the 70% shade treatment. Similarly, two of these measurements (THW and EPW) scaled with isometry in the 30% shade treatment, and MPW scaled with positive allometry. Isometry in trabecular horn width (THW) and ethmoid process width (EPW) may be functionally related to diet composition and feeding behavior. The suprarostral cartilages attach to the trabecular horns and function as the movable upper jaw in tadpoles (Cannatella 1999). Since this upper jaw element is repeatedly used in rasping substrates, it may be beneficial to maintain isometry in THW as the organism grows in order to provide a robust structural component for attachment. Likewise, the trabecular horns extend forward from the ethmoid (Cannatella 1999); thus, isometry in EPW may reflect the need for providing additional structural support to the trabecular horns. Isometric growth in SRA (the distance between the articulations of the suprarostral cartilages to the trabecular horns) suggests that specimens from the 70% shade treatment possessed proportionally wider suprarostral cartilages than specimens from the other shade treatments. If so, specimens from the 70% shade would possess a proportionally greater surface for rasping substrates.

The muscular process of the palatoquadrate is one of the most prominent features of the larval anuran chondrocranium. This process serves as an attachment site for the orbitohyoideus and suspensoriohyoideus muscles (Cannatella 1999) (Fig. 8).

Electromyographic data indicate that in *Rana catesbiana* the orbitohyoideus is always active during rasping feeding and is either entirely inactive, or produces only low amplitude bursts of activity, during normal gill irrigation (Larson and Reilly 2003). Therefore, positive allometry and isometry observed in MPW for specimens from the 30% and 70% shade treatments suggest that persistent rasping feeding throughout ontogeny generating enlarged orbitohyoideus musculature which subsequently affects MPW.

The scaling relationship of the length of the articular process of the palatoquadrate (PAQL) may be of functional importance as well. This portion of the palatoquadrate serves as an attachment site for the primary jaw depressor muscles (hyoangularis, quadratoangularis, and suspensorioangularis; Cannatella 1999; Fig. 8). As these muscles contract they create tension in the mandibulo-suprarostral ligament, which causes the upper jaw to open (Cannatella 1999). By maintaining isometry in PAQL, as opposed to negative allometry as is typically predicted, these tadpoles would develop a large gape and possibly be able to generate greater rasping forces.

Geometric Morphometrics

Canonical variates analysis indicated that specimens from the three shade treatments were significantly different in terms of their chondrocranial morphology. This was true for both the ontogenetic and terminal shape datasets. Moreover, the terminal shape specimens appeared to exhibit a greater degree of morphological divergence. This suggests that prolonged exposure to a particular light intensity treatment exacerbated the effects of that treatment on morphology.

Few studies have assessed the effects of environmental conditions on the morphology of the larval anuran chondrocranium. Larson (2004) was the first to suggest that biological factors may influence chondrocranial shape, after documenting considerable intraspecific chondrocranial shape variation in *Bufo americanus* tadpoles. Recent investigations have revealed that temperature (Jorgensen and Sheil 2008), and diet composition (Chapter 1) may also generate morphological variation in the larval anuran chondrocranium. This study demonstrated that light intensity, in addition to influencing size and developmental time, can significantly affect morphology in a variety of ways. The results presented here further demonstrate the malleable nature of larval anurans in the face of environmental heterogeneity. Additional investigations are needed to identify other potential causes of intraspecific variation in chondrocranial morphology. Quantifying more precisely how larval shape variation influences reproductive fitness in adult anurans would be very informative as to the ultimate costs of larval habitat. If shape variation in the larval stages results in post-metamorphic shape variation, there may be disparities in performance due to conditions of the larval environment.

Table 6. Results of one-way ANOVAs on within treatment log10 SVL

Gosner Grouping	0% Shade		30% Shade		70% Shade	
Early	$F_{3,28}$= 1.66	p= 0.20	$F_{3,27}$= 0.302	p= 0.82	$F_{3,35}$= 0.966	p= 0.42
Middle	$F_{3,28}$= 1.72	p= 0.18	$F_{3,30}$= 0.772	p= 0.52	$F_{3,33}$= 0.634	p= 0.60
Late	$F_{3,20}$= 0.729	p= 0.55	$F_{3,19}$= 0.747	p= 0.54	$F_{3,8}$= 1.66	p= 0.25

Table 7. Mean SVL and developmental time (± 1 SE) for specimens from the shade treatments at early, middle, and late developmental stages.

	Early Development (28-31)			Middle Development (32-35)			Late Development (32-35)		
	n	SVL	Days	n	SVL	Days	n	SVL	Days
0%	32	7.77± 0.34	23.41± 1.50	32	8.52± 0.31	27.69± 2.05	24	9.34± 0.29	28.54± 2.60
30%	31	7.32± 0.19	33.77± 1.95	33	8.78± 0.17	45.82±3.93	23	10.85± 0.28	46.62±3.57
70%	39	7.34± 0.13	55.15± 3.79	37	8.71± 0.21	67.97±4.36	12	10.54± 0.49	76.5± 6.80

Table 8. Results of reduced major axes regressions of linear measurements of the chondrocrania against SVL. Confidence limits that overlap the value k =1 indicate isometry, whereas confidence limits that fall below or above a value of k =1 indicate negative and positive allometry, respectively. Differences in scaling patterns are indicated by (Ω) -different from 0%, (*)- different from 30%, (†)- different from 70%.

	Measurement	Intercept	Slope	R2	95% LCL	95% UCL	Scaling
0% Shade	PAQL	-0.8851	0.7546	0.3075	0.6198	0.8894	Negative Allometry †
	THL	-0.8317	0.82	0.03827	0.6474	0.9926	Negative Allometry
	SRA	-0.5485	0.6094	0.3109	0.5008	0.7179	Negative Allometry †
	PAQO	-0.1225	0.5359	0.3035	0.4399	0.6319	Negative Allometry
	THW	-1.419	0.9102	0.2414	0.7401	0.9864	Negative Allometry*†
	EPW	-0.8921	0.6751	0.2085	0.5462	0.8039	Negative Allometry*†
	MPW	-0.9801	0.8431	0.3267	0.6946	0.9915	Negative Allometry*†
	CAW	-0.1106	0.642	0.2712	0.5244	0.7597	Negative Allometry
	BCPQ	-0.5672	0.71	0.2584	0.5788	0.8412	Negative Allometry
	MW	0.00059	0.6019	0.2755	0.492	0.7119	Negative Allometry
	OCL	-0.474	0.5604	0.2084	0.4534	0.6673	Negative Allometry
	BCL	-0.109	0.6357	0.3093	0.5223	0.7419	Negative Allometry
30% Shade	PAQL	-0.8829	0.8003	0.5202	0.6806	0.92	Negative Allometry †
	THL	-0.8077	0.8384	0.2519	0.6819	0.9949	Negative Allometry
	SRA	-0.6799	0.7925	0.615	0.6864	0.8987	Negative Allometry †
	PAQO	-0.2547	0.7146	0.5896	0.6158	0.8134	Negative Allometry
	THW	-1.446	0.9675	0.2546	0.7872	1.148	IsometryΩ
	EPW	-1.256	1.099	0.4889	0.9293	1.269	Isometry
	MPW	-1.502	1.428	0.6977	1.259	1.598	Positive Allometry †Ω
	CAW	-0.1975	0.7716	0.6519	0.6733	0.8699	Negative Allometry
	BCPQ	-0.6118	0.8157	0.5107	0.6926	0.9389	Negative Allometry
	MW	-0.1103	0.7685	0.6107	0.665	0.872	Negative Allometry
	OCL	-0.7265	0.8541	0.4824	0.7215	0.9868	Negative Allometry
	BCL	-0.2482	0.8055	0.6535	0.7032	0.9079	Negative Allometry
70% Shade	PAQL	-1.023	0.9553	0.6812	0.8395	1.071	Isometry*Ω
	THL	-0.7669	0.8048	0.3245	0.6629	0.9467	Negative Allometry
	SRA	-0.9027	1.036	0.6516	0.9047	1.67	Isometry*Ω
	PAQO	-0.2744	0.7286	0.6666	0.6383	0.8189	Negative Allometry
	THW	-1.658	1.179	0.3773	0.9797	1.397	IsometryΩ
	EPW	-1.283	1.117	0.5357	0.9535	1.28	Isometry
	MPW	-0.9611	0.9549	0.5671	0.82	1.09	Isometry*Ω
	CAW	-0.1856	0.7539	0.6696	0.6609	0.8469	Negative Allometry
	BCPQ	-0.6725	0.8704	0.65	0.7599	0.9808	Negative Allometry
	MW	-0.1177	0.7584	0.7178	0.672	0.8449	Negative Allometry
	OCL	-0.7313	0.86	0.6479	0.7505	0.9695	Negative Allometry
	BCL	-0.2766	0.8198	0.718	0.7264	0.9132	Negative Allometry

Figure 9. Photograph of mesocosms representing all three treatments used in this study (foreground: 0% shade, top left: 70% shade, top right: 30% shade). The small white squares in each pool are ceramic tiles that were used to quantify periphyton communities. Temperature data loggers (1/pool) were sealed inside the white cylinders.

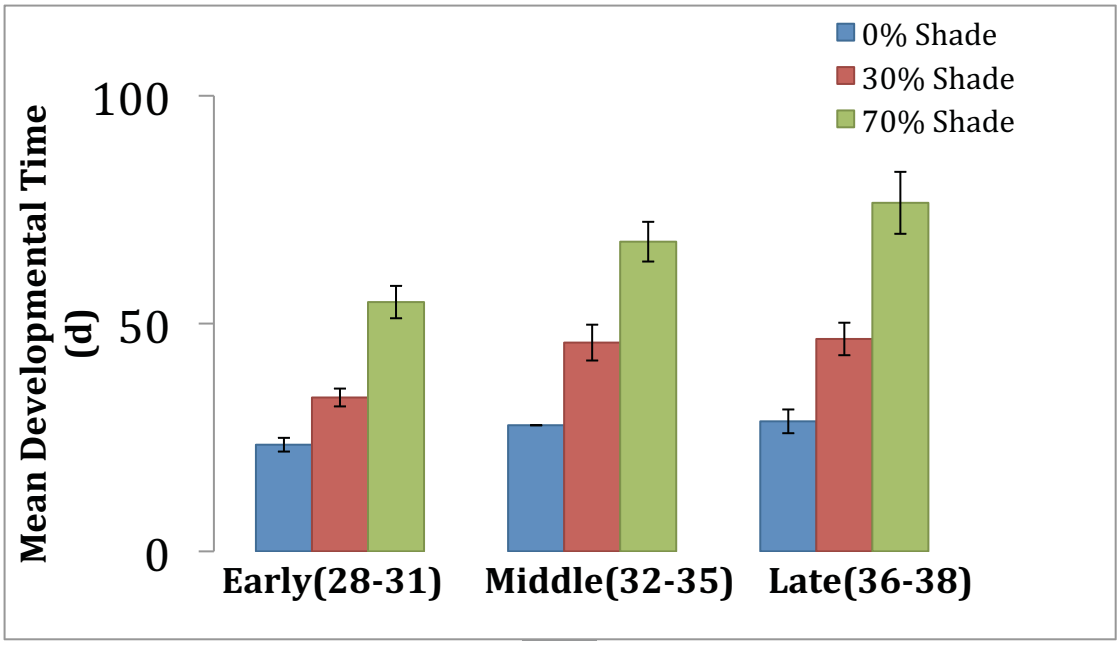

Figure 10. Mean developmental time (d) for specimens from all three shade treatments at early, middle, and late Gosner stages.

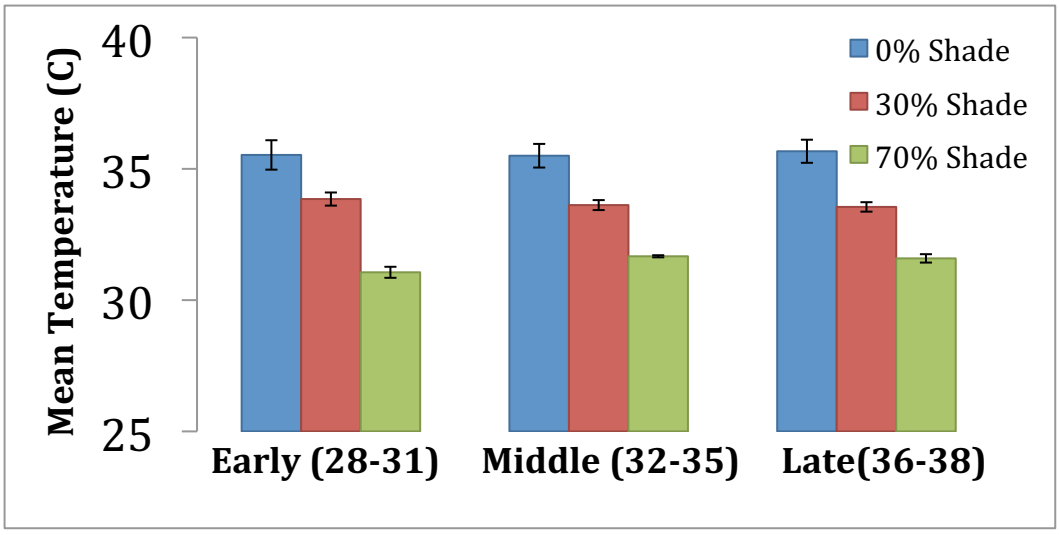

Figure 11. Mean temperature (˚C) of pools from the three shade treatments. Temperatures shown are the average of all the temperatures recorded between 1pm and 7pm until the date that corresponds with the average time to development for early, middle, and late stage specimens from each treatment. Temperatures were significantly different during the average time periods for specimens to reach early, middle, and late developmental stages (Kruskal-Wallis: early: $X^2 = 60.26$, df = 2, p = < 0.0001; middle: $X^2 = 40.82$, df = 2, p = < 0.0001; late: $X^2 = 40.74$, df = 2, p = < 0.0001).

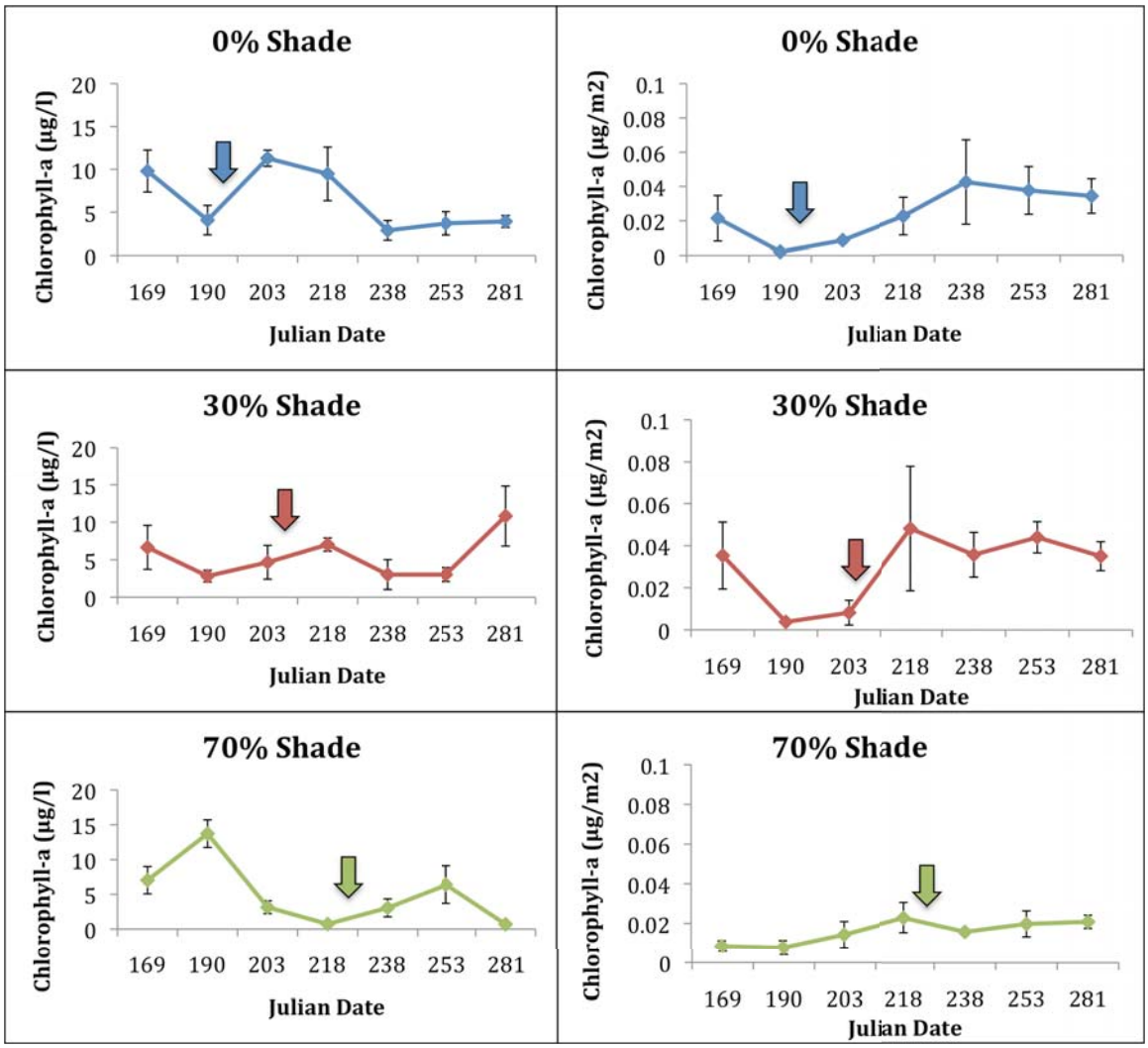

Figure 12. Average chlorophyll a concentrations of phytoplankton (left side) and periphyton (right side) throughout the experiment. Lines on each graph were constructed by taking the average chlorophyll a concentration of all the pools within a treatment. The arrows indicate the average time to late developmental stages for specimens from that treatment.

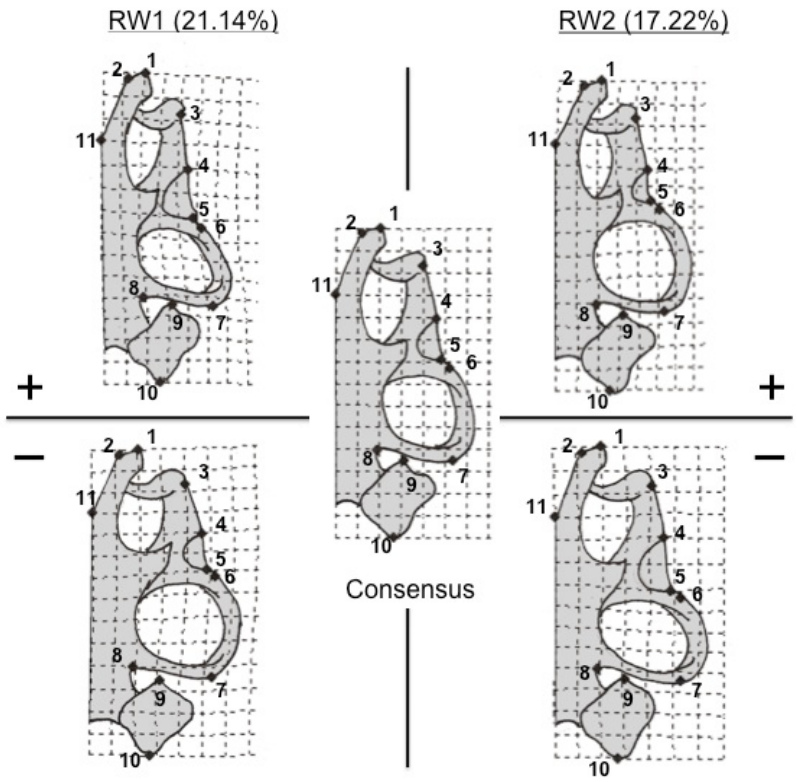

Figure 13. .Thin-plate spline deformation grids depicting chondrocranial shape change (relative to consensus form) throughout larval development (whole ontogeny). At the center is the consensus form, the left side shows positive (above) and negative extremes along the first relative warp (RW) axis, and the right side shows positive and negative extremes along the second RW axis. Outlines facilitate visualization of shape change, and do not represent a particular specimen.

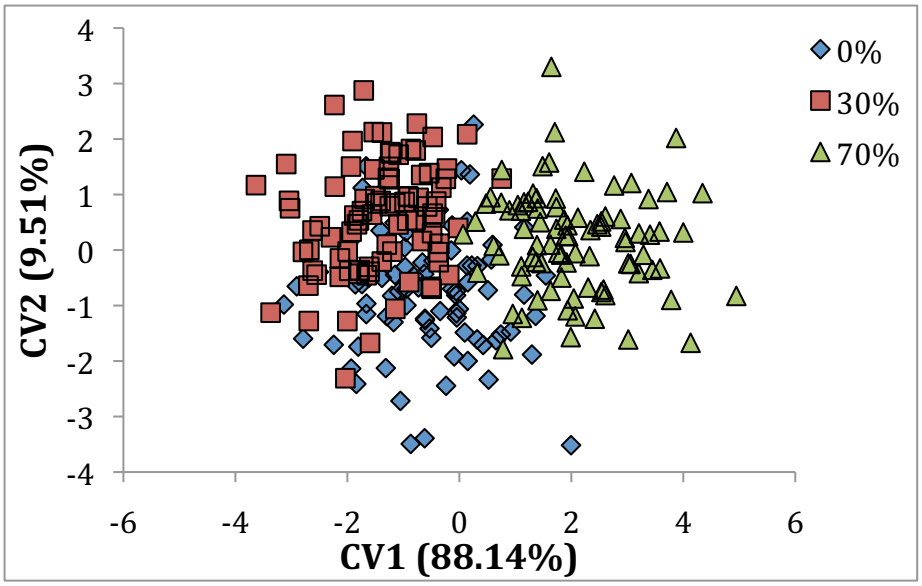

Figure 14. Scatterplot of specimen scores (n=264) along canonical variate axes throughout larval development (whole ontogeny). The first CV axis separates specimens raised in the 70% shade from those raised in 30% and 0% shade treatments. Specimens from the 0% shade treatment generally scored lower on the CV2 axis.

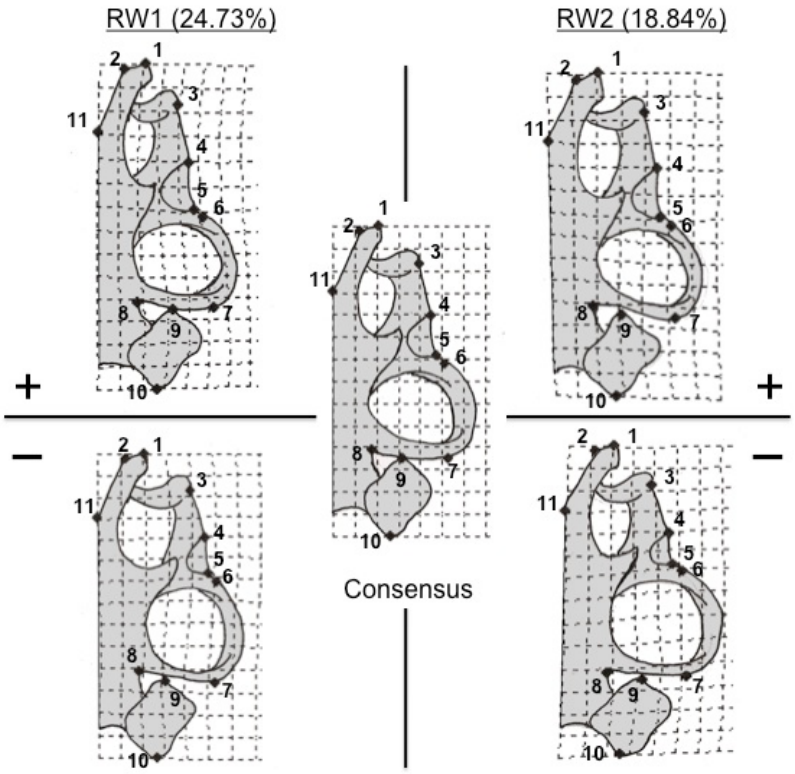

Figure 15. Terminal Shape. Thin-plate spline deformation grids depicting chondrocranial shape change (relative to consensus form) at positive and negative extremes along the first two relative warp axes. At the center is the consensus form, the left side shows positive (above) and negative extremes along the first RW axis, and the right side shows positive and negative extremes along the second RW axis. Outlines are only meant to facilitate visualization of shape change, and do not represent a particular specimen.

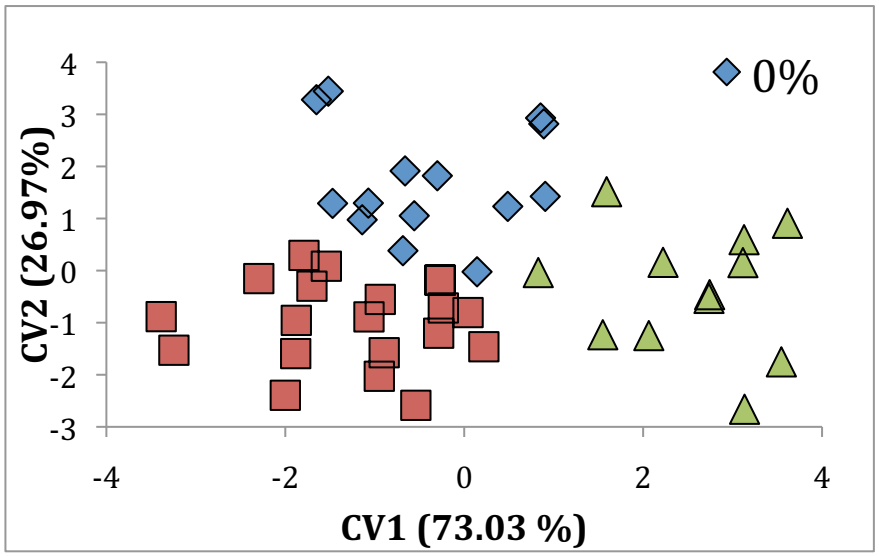

Figure 16. Terminal Shape. Scatterplot of specimens (n=48) CV1 and CV2 scores. The first CV axis explained 73.03% of the variation in the data and appears to separate specimens raised in the 70% shade from those raised in 30% and 0% shade treatments. The second CV axis explained 26.97% of the variance and separates specimens from the 0% and 30% shade treatments. Green squares represent specimens from the 70% shade treatment, blue dot represent specimens from the 30%, and yellow boxes represent 0% shade specimens.

References

Álvarez D, Nicieza AG. 2002. Effects of temperature and food quality on anuran larval growth and metamorphosis. *Functional Ecology* 16, 640-648.

Altig R, Whiles MR, Taylor CL. 2007. What do tadpoles really eat? Assessing the trophic status of an understudied and imperiled group of consumers in freshwater habitats. Freshwater Biology 52:386-395.

Arar. E.J. and Collins, G.B. 1997. Method 445.0, *In Vitro* Determination of Chlorophyll *a* and Pheophytin *a* in Marine and Freshwater Algae by Fluorescence. *In* Methods for the Determination of Chemical Substances in Marine and Estuarine Environmental Matrices, 2nd Edition. National Exposure Research Laboratory, Office of research and development, USEPA., Cincinnati, Ohio (EPA/600/R-97/072, Sept. 1997).

Ashton RE, Ashton PH. 1988. Handbook of Amphibians and Reptiles of Florida: Part Three: The Amphibians. Miami: Windward Publishing.

Atkinson D. 1996. Ectotherm life history responses to developmental temperature. Animals and Temperature: Phenotypic and evolutionary adaptations. Eds. I.A. Johnston & A.F. Bennett. Cambridge University Press, Cambridge.

Bernays, EA. 1986. Diet-Induced Head Allometry among Foliage-Chewing Insects and its Importance for Graminivores. *Science* 231: 495-497.

Berven KA. 1990. Factors affecting population fluctuation in the larval and adult stages of the wood frog (*Rana sylvatica*). Ecology71:1599-1608.

Birch, LL. 1999. Development of food preferences. *Annual Review of Nutrition* 19: 41-62.

Bookstein FL. 1991. Morphometric Tools for Landmark Data. Cambridge: Cambridge University Press.

Bookstein FL. 1996. Standard formula for the uniform shape component in landmark data. In: Marcus LF , CM, Loy A, Naylor G, Slice DE, ed. Advances in Morphometrics. Proceedings of the 1993 NATO Advanced Studies Institute on Morphometrics in Il Ciocco, Italy. New York: Plenum, p.153-168.

Cannatella D. 1999. Architecture:cranial and axial musculoskeleton. In: McDiarmid RW, Altig R, ed. Tadpoles: the biology of anuran larvae. Chicago: University of Chicago Press

Castaneda LE, Sabat P, Gonzalez SP, Nespolo RF. 2006. Digestive Plasticity in Tadpoles of the Chilean Giant Frog (Caudiverbera caudiverbera): Factorial Effects of Diet and Temperature. Physiological and Biochemical Zoology 79:919-926.

Death RG, Zimmermann EM. 2005. Interaction between disturbance and primary productivity in determining stream invertebrate diversity. Oikos 111:392-402.

Dickman M. 1968. The effect of grazing by tadpoles on the structure of a periphyton community. Ecology 49:1188-1190.

Dingerkus G, Uhler LD. 1977. Enzyme Clearing of Alcian Blue Stained Whole Small Vertebrates for Demonstration of Cartilage. *Biotechnic and Histochemistry* 52: 229 - 232.

Emerson SB, Bramble D. 1993. Scaling, allometry, and skull design. In: Hanken J , Hall B, ed. The skull. Functional and evolutionary mechanisms. Chicago: University of Chicago Press. p 384-421.

Etkin W. 1968. Hormonal control of amphibian metamorphosis. In Physiology of the Amphibia. Vol. 1. Edited by J.A. Moore. London: Academic Press

Felsenstein, J. 1985. Phylogenies and the Comparative Method. *The American Naturalist* 125: 1.

Gibbons JW, Semlitsch RD. 1991. Guide to the reptiles and amphibians of the Savannah river site. Athens: University of Georgia Press.

Gosner KL. 1960. *A simplified table for staging anuran embryos and larvae with notes on identification*. New York Herpetological Society, New York.

Gould SJ. 1966. Allometry and size in ontogeny and phylogeny. *Biological Reviews* 41: 587-638.

Gradwell N. 1972. Gill irrigation in *Rana catesbiana*. II. On the muskuloskeletal mechanism. Can J Zool. 50:501-521.

Harvey PH, Pagel MD. 1991. The comparative method in evolutionary biology. New York: Oxford University Press.

Herring SW. 1993. Epigenetic and functional influences on skull growth. In: Hanken J, Hall B, ed. The skull, Development. Chicago: Chicago University Press.

Hochachka PW, Somero G. 1984. Biochemical Adaptation. Princeton:Princeton University Press.

Hoff KS, Blaustein AR, McDiarmid RW, Altig R. 1999. Behavior: Interactions and their consequences. In: McDiarmid RW, Altig R, ed. Tadpoles: the biology of anuran larvae. Chicago: University of Chicago Press.

Jorgensen ME, Sheil CA. 2008 Effects of Temperature Regime Through Premetamorphic Ontogeny on Shape of the Chondrocranium in the American Toad, *Anaxyrus americanus*.

The Anatomical Record: Advances in Integrative Anatomy and Evolutionary Biology 291:818-826.

Larson PM. 2002. Chondrocranial development in larval *Rana sylvatica* (Anura: Ranidae): Morphometric analysis of cranial allometry and ontogenetic shape change. *Journal of Morphology* 252: 131-144.

Larson, PM. 2004. Chondrocranial morphology and ontogenetic allometry in larval *Bufo americanus* (Anura, Bufonidae). *Zoomorphology* 123: 95-106.

Larson PM. 2005. Ontogeny, phylogeny, and morphology in anuran larvae: Morphometric analysis of cranial development and evolution in *Rana tadpoles* (Anura: Ranidae). *Journal of Morphology* 264: 34-52.

Larson PM, Reilly SM. 2003. Functional morphology of feeding and gill irrigation in the anuran tadpole: electromyography and muscle function in larval *Rana catesbeiana*. *Journal of Morphology* 255: 202-214.

Laugen AT, Laurila A, Räsänen K, Merilä J. 2003. Latitudinal countergradient variation in the common frog (*Rana temporaria*) development rates; evidence for local adaptation. Journal of Evolutionary Biology 16:996-1005.

Lock MA, Wallace RR, Costerton JW, Ventullo RM, Charlton SE. 1984. River epilithon: toward a structural and functional model. Oikos 42:10-22.

Marian MP, Pandian TJ. 1985. Effect of temperature on development, growth and bioenergetics of the bullfrog tadpole *Rana tigrina*. Journal of Thermal Biology 10:33 157-161.

McDiarmid RW, Altig R. (eds.) 1999. Tadpoles: The biology of anuran larvae. Chicago: University of Chicago Press, 1999.

Merila J, Sheldon BC. 2000. Lifetime Reproductive Success and Heritability in Nature. The American Naturalist 155:301-310.

Mittelbach, GG, Osenberg CW, Wainwright PC. 1992. Variation in resource abundance affects diet and feeding morphology in the pumpkinseed sunfish (Lepomis gibbosus). *Oecologia* 90: 8-13.

Monteiro LR. 1999. Multivariate regression and geometric morphometrics: the search for causal factors in the analysis of shape. Syst Biol 48:192-199.

Monteiro LR, Abe SA. 1999. Functional and historical determinants of shape in the scapula of Xenarthran mammals: Evolution of a complex morphological structure. Journal of Morphology 241:251-263.

Moran NA. 1992. The Evolutionary Maintenance of Alternative Phenotypes. *The American Naturalist* 139: 971.

Morin A, Lamourex W, Busnarda J. 1999. Empirical models predicting primary productivity from chlorophyll a and water temperature for stream periphyton and lake and ocean phytoplankton. Journal of the North American Benthological Society 18: 299-307

Relyea RA. 2000. Trait-mediated indirect effects in larval anurans: reversing competition with the threat of predation. *Ecology* 81: 2278-2289.

Relyea RA. 2001. Morphological and behavioral plasticity of larval anurans in response to different predators. Ecology;82:523-540.

Relyea RA. 2003. How prey respond to combined predators: a review and an empirical test. Ecology;84:1827-1839.

Relyea RA, Auld JR. 2004. Having the guts to compete: how intestinal plasticity explains costs of inducible defences. *Ecology Letters* 7: 869-875.

Relyea RA, Auld JR. 2005. Predator- and competitor-induced plasticity: how changes in foraging morphology affect phenotypic trade-offs. *Ecology* 86: 1723-1729.

Rholf FJ, Loy A, Corti M. 1996. Morphometric analysis of the old world Talpidae (Mammalia, Insectivora) using partial warp scores. Syst Biol;45:344-362.

Schiesari L. 2006. Pond canopy cover: a resource gradient for anuran larvae. Freshwater Biology 51:412-423.

Seale D. 1980. Influence of Amphibian Larvae on Primary Production, Nutrient Flux, and Competition in a Pond. Ecology 61:1531-1552.

Seale DB, Beckvar N. 1980. The comparative ability of Anuran larvae (Genera: *Hyla*, *Bufo* and *Rana*) to ingest suspended blue-green algae. Copeia 1980: 495-503.

Semlitsch RD, Scott DE, Pechmann JHK. 1988. Time and size at metamorphosis related to adult fitness in Ambystoma talpoideum. Ecology 69:184-192.

Smith DC, Van Buskirk J. 1995. Phenotypic Design, Plasticity, and Ecological Performance in Two Tadpole Species. The American Naturalist;145:211.

Smith-Gill SJ, Berven KA. 1979. Predicting amphibian metamorphosis. American Naturalist 113:563-585.

Swennen C, DeBruun LLM, Duiven P, Leopold MF, Marteun ECL. 1983. Differences in bill form of the oystercatcher *Haematopus ostralegus*, a dynamic adaptation to specific foraging techniques. Netherlands J of Sea Research;17:57-83.

Thompson DK. 1992. Consumption rates and the evolution of diet-induced plasticity in the head morphology of of *Melanoplus femurrubrum* (Orthoptera: Acrididae). Oecologia;89:204-213.

Thurgate NY, Pechman JK. 2007. Canopy Closure, Competition, and the Endangered Dusky Gopher Frog. Journal of Wildlife Management 2007:1845-1852.

Trowbridge CD. 1991. Diet specialization limits herbivorous sea slug's capacity to switch among food species. Ecology;72:1880-1888.

Trowbridge CD. 1997. Dietary induction of Opisthobranch morphology: *Placida dendritica* (Alder & Hancock) on different green algal hosts. J. Moll. Stud. 63:29-38.

Ultsch GR, Bradford DF, Freda J. 1999. Ecological physiology of tadpoles. In: McDiarmid RW, Altig R, eds. Tadpoles: The Biology of anuran larvae. Chicago: University Chicago Press.

Via S, Lande R. 1985. Genotype-environment interaction and the evolution of phenotypic plasticity. Evolution 39:505-522.

Wainwright PC, Osenberg CW, MittleBach GG. 1991. Trophic polymorphism in the pumpkinseed sunfish (*Lepomis gibbosus* Linnaeus): effects of environment on ontogeny. Ecology;5:40-55.

Wassersug RJ, Hoff KS. 1979. A comparative study of the buccal pumping mechanism of tadpoles. *Biological Journal of the Linnean Society* 12: 225-259.

Werner EE, Glennemeier KS. Influence of Forest Canopy Cover on the Breeding Pond Distributions of Several Amphibian Species. Copeia 1999:1-12.

Wright AH, Wright AA. 1949. Handbook of Frogs and Toads of the United States and Canada. Third Edition ed. Ithaca: Comstock Publishing Associates.

Appendix A

Enzyme Clearing and Cartilage Staining Methodology

It should be noted that the procedure described here is a modified version of the protocol in the following article: **Dingerkus G, and Uhler LD. 1977. Enzyme clearing of alcian blue stained whole small vertebrates for demonstration of cartilage. Stain Technol 52:229-232.** These methods were developed to clear and stain larval *Bufo terrestris* ranging in development from Gosner 28- 38. Because of interspecific size variation among species of larval anurans, some modification of this protocol may be necessary when attempting to achieve the same results with a species other than *B. terrestris*.

Methods

1. Specimens are fixed in 10% formalin for several days.
2. Wash specimens in three changes of deionized H_2O, allowing the specimens to spend approximately 18 to 24 hours in each wash. Contrary to Dingerkus and Uhler (1977), and Wassersug (1976), skinning and eviscerating each specimen is unnecessary for *B. terrestris*. Anecdotally, I have attempted to clear and stain larger tadpoles (*Rana Catesbiana,* > 50mm SVL) without skinning them and was unsuccessful, as their tissue would not clear.
3. Place specimens into a mixture of 10 mg Alcian Blue 8GX, 80 ml of 95% ethyl alcohol, and 20 ml of glacial acetic acid for 24- 36 hours. This step is especially important because if the above dye solution is too strong you will overstain your specimens, likewise if the dye is not strong enough then you will understain them which may prevent you from viewing cartilaginous structures in their entirety. As

a rule of thumb, make sure that you can see your hand through the solution if you hold it up behind the flask.

4. Transfer specimens through the following series of alcohol changes: 95%, 70%, 40%, and 15%. Specimens should remain in each alcohol solution for no less than three hours.
5. Transfer specimens to deionized water for a minimum of three hours.
6. Place specimens in an enzyme solution of 70 ml deionized water, 30 ml aqueous sodium borate, and 1 gm of trypsin enzyme. Watch specimens carefully during this step as overdigestion could potentially ruin them. With smaller species (e.g. *Bufo terrestris*) 24 hours is plenty of time, whereas larger species (e.g. *Rana catesbiana*) may require up to 36 hours. Regardless of species, specimens should be removed once they go limp.
7. Briefly rinse specimens in deionized water (a few minutes will do), and then transfer to a 0.5% aqueous KOH solution to which enough Alizarin Red dye has been added to give the solution a deep purple color. This step only takes 24 hours, and overstaining is not as much of a concern as it is with step # 3. However, the KOH used in this solution is fairly strong and leaving specimens in solution for over 48 hours could result in damage.
8. Transfer specimens through a 0.5% KOH- Glycerin series of 1.) ¾ KOH- ¼ Glycerin, 2.) ½ KOH- ½ glycerine, and 3.) ¼ KOH- ¾ Glycerin. At this point pigment will still be present in your specimens and therefore H_2O_2 will need to be added to complete the bleaching of the dark pigment. The H_2O_2 presents somewhat of a tradeoff in that if you add a large quantity (e.g. 4 drops per

specimen) the specimens will clear rapidly and completely, however the H_2O_2 will also cause bubbles to form in their tissues, which can severely increase handling time when you attempt to photograph the specimens for morphological purposes. From personal experience, the best way to apply H_2O_2 in this step is to add 1-2 drops per specimen (depending on the amount of dark tissue present) while the specimens are in the first step of the KOH- Glycerin series. Specimens may then be left until substantial clearing has occurred (this may take anywhere from 5- 48 hours depending upon the specimen). While in the last 2 stages of the KOH- Glycerin series 1-2 additional drops of H_2O_2 may be added if further clearing is necessary. The amount of time specimens spend in the last two KOH-Glycerin stages depends mainly on how clear they are. If the desired level of clearing has occurred after the first addition of H_2O_2 , then 5 hours in the ½- ½ , and 5 hours in the ¼- ¾ solution is all that is necessary.

9. Transfer specimens to pure Glycerin to which a few crystals of Thymol have been added to inhibit the growth of mold and bacteria.

Appendix B

A method for constructing an adjustable platform to obtain lateral photographs of larval anurans

Digitally photographing specimens and using computer software to obtain morphological measurements is a commonly used technique in larval anuran research. Lateral photographs of specimens can be used to obtain measures such as snout-vent length, body height, tail length, tail height, tail musculature length, and tail musculature height (Dayton et al. 2005; Lardner 2000; Relyea 2001). However, obtaining quality lateral photographs of larval anurans can be difficult due to their general body plan (a rounded body and laterally compressed tail).

When a specimen is laid on its side in a lateral view, the tail remains in a flat plane, however, the curvature of the body often causes the specimen to bend so that the body and tail are no longer aligned in a flat plane (Fig. 1A and 1B). If the specimen is bent when photographed, measurements of total length or snout-vent length are likely to be underestimates (Fig. 1B). Thus, it is necessary to compensate for the lateral curvature of the body in order to maximize the accuracy of measurements obtained from lateral photographs.

McDiarmid and Altig (1999) describe a modified aquarium apparatus for photographing larval anurans for voucher or identification purposes. However, because morphological studies often require large sample sizes, decreasing the amount of time it takes to prepare a specimen for photographing is important for efficiency purposes. We describe a simple method for constructing an adjustable platform that enables researchers to consistently and rapidly obtain quality lateral photographs of formalin fixed tadpoles. This platform supports specimens in a manner that prevents bending caused by the lateral

curvature of the body (Fig. 1C and 1D), and can accommodate specimens of varying sizes.

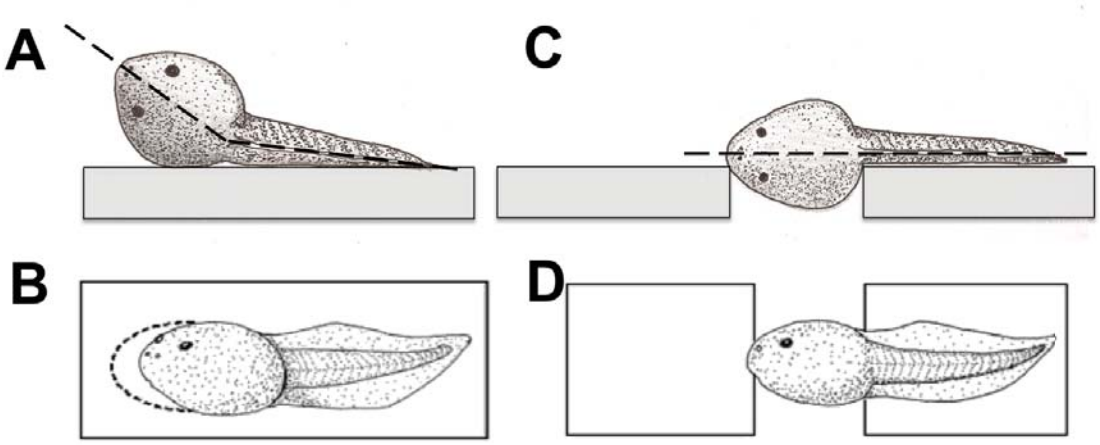

Fig. 1. (A) Side view illustration showing the bending of a specimen caused by the lateral curvature of the body. The dashed line is provided to enhance visualization of the degree of bending. (B) Specimen A, viewed from above. The dashed line shows where the outline of the head would be if the specimen's body and tail were aligned in a flat plane. (C) Side view of a specimen supported in a manner that prevents the lateral curvature of the body. (D) Specimen C when viewed from above.

Platform construction can be completed in less than 30 minutes with the following materials: 2 microscope slides (3 in x 1 in), two hollow tubes, one with a slightly larger diameter than the other (we used a drinking straw and the shaft of a disposable ink pen), and epoxy glue. Microscope slides (3 in x 1 in) are used as a platform on which the

specimen rests. The hollow tubes will be glued beneath the microscope slides, and will allow the platform to be adjusted. A drinking straw (or tube with the smaller diameter) is cut into two 4 inch pieces, which are glued parallel to the short edge of the slide approximately one-half inch from each end. The pieces of straw should also protrude at least one-half inch from the long edge of the microscope slide. The hollow cylinders of disposable ink pen shafts (or the tube with the greater diameter) are then glued to the second microscope slide in the same manner as previously described, with the exception that the circular openings of the shafts should not protrude outwards from underneath the microscope slide (Fig. 2A). The microscope slides are aligned and the two pieces of drinking straw are inserted into the ink pen shafts. The larger diameter of the disposable ink pen allows the stage to be manipulated to accommodate specimens of different sizes. A scale bar can be glued to the surface of either microscope slide so long as it will be in the field of view with the specimen when it is photographed from directly above (Fig 2B). Specimens are positioned on the platform so that only the extreme anterior of the body is touching the slide on the left, and the tail is supported by the slide on the right (Fig 1C, 1D, and Fig.2B). From the author's experience, handling time for each specimen is less than 20 seconds.

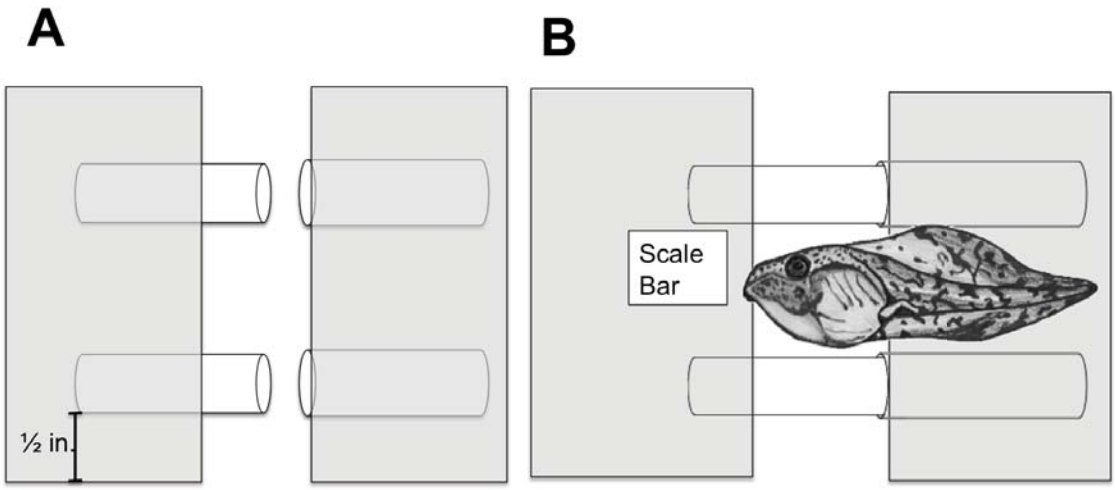

Fig. 2. (A) Pieces of drinking straw (left), and hollow ink pen shafts (right) secured to the microscope slides. (B) Specimen properly positioned on the finished platform.

We have found this apparatus to be both durable and efficient as it has been used to obtain over 500 photographs of specimens, with an approximate handling time of under 20 seconds for each specimen. Further, this platform to be especially useful when photographing smaller species of larval anurans (e.g. *Bufo terrestris* < 40 mm total length), or specimens at earlier developmental stages. Simple modifications such as adding an additional microscope slide to each side of the platform may be necessary in order to photograph specimens from larger species (i.e. *Rana catesbeiana*) or later developmental stages.

Literature Cited

Dayton, G. H., D. Saenz, K. A. Baum, R. B. Langerhans, and T. J. Dewitt. 2005. Body shape, burst speed and escape behavior of larval anurans. Oikos 111: 582-591

Lardner, B. 2000. Morphological and life history responses to predators in larvae of seven anurans. Oikos 88: 169-180

Relyea, R. A. 2001. Morphological and behavioral plasticity of larval anurans in response to different predators. Ecology. 82(2): 523-540

Appendix C

Notes on Obtaining Dorsal Photographs of the Chondrocranium

After the clearing and staining process is completed some dissection is required in order to prepare specimens to be photographed. First, the chondrocrania must be detached from the rest of the body. This is a simple process that can be done underneath a dissecting scope using a pair of microdissection scissors and forceps to manipulate the specimen. The easiest way to do this is to cut the spinal column just posterior to the base of the chondrocranium, and then follow that incision around the body in a transverse fashion until the chondrocranium is detached from the body. Doing this allows the chondrocranium to rest in a flat plane when viewed from above, and it also enhances visualization because the gut contents (which typically do not clear) are no longer in close proximity to the chondrocranium. For most specimens this is all the dissection needed, however, occasionally in larger specimens or specimens that have been heavily stained much of the branchial basket is visible underneath the chondrocranium, which can impair visibility from above. When necessary, the branchial basket can be removed by cutting through the cartilage that attaches it to the chondrocranium just beneath the muscular process of the palatoquadrate.

Once any necessary dissection was completed, I placed the detached chondrocranium inside half of a small watch glass with a scale bar inside of it. Using a dissecting scope, I positioned the chondrocranium so that it could be viewed next to the scale bar when photographed. Because the clearing and staining process requires the use of hydrogen peroxide, it is inevitable that small air bubbles will form in the tissue of specimens. When the bubble(s) occur in close proximity to a particular structure of

interest they need to be removed prior to photographing. From my experience, there is no right or wrong way to get rid of the bubbles, most of the time simply prodding the bubbles with a thin needle will pop them or move them out of the way. However, in some cases, if the bubble is deep within the tissue prodding and poking will not work and it is necessary to make a small incision so that the bubble can be popped or forced out of the tissue. When attempting to eliminate bubbles it is important to handle the specimen with great care because of fragility of the chondrocranium and the fact that disarticulation could make specimens useless. After properly positioning the chondrocranium and resolving any issues associated with bubbles, I placed the watch glass (with the chondrocranium and scale bar) on top of a light table and photographed the chondrocranium with a digital camera positioned directly above the watch glass.

Appendix D

Phytoplankton Sampling Methods

1. I collected subsurface (approximately 2 in. beneath the surface) water samples in 500 ml plastic bottles
2. I filtered 100 ml of each sample through a Whatman GF/F glass fiber filter, and stored the filters in a dark freezer until chlorophyll could be extracted.
3. In order to extract chlorophyll from the filters I placed them in 8 ml of 90% acetone for 24 hours and stored them in a dark refrigerator.
4. After 24 hours of extraction, samples were removed from the refrigerator and allowed to warm to room temperature for 30 minutes. I the removed the filters from the 13 x 100 mm test tubes used for extraction and then placed the 8 ml of solution in the fluorometer to obtain a reading of the chlorophyll-a concentration. After each initial reading I added three drops of 0.5 M HCL to acidify the sample and then placed the sample back in the fluorometer to determine pheophyton-a concentrations of the sample.
5. In several samples the chlorophyll-a concentration of the sample was too high for the fluorometer to obtain an accurate reading. In these instances I diluted the sample by 50% (4 ml of sample: 4 ml of 90% acetone).
6. After collecting data from all of the samples, I used the following formulae to determine the concentrations of chlorophyll-a and pheophyton-a in µg/L:

   Step 1:
   chlorophyll-a µg/L = $(r / r - 1) (R_b - R_a)$

   pheophyton-a µg/L = $(r / r - 1) (rR_a - R_b)$

Step 2:
[value from Step 1 x extraction volume (ml)] ÷ volume of sample filtered (ml)

*where:
r = 2.08 (before/after standard calibration)
R_b = sample reading before adding acid
R_a = sample reading after adding acid

Appendix E

Periphyton Sampling Methods

1. I collected ceramic tiles from the pools and returned them to the lab where I scraped all of the organic material growing on the tiles off with a razorblade. The material from each tile was then filtered through a Whatman GF/F glass fiber filter and the filters were stored in a dark freezer until chlorophyll was extracted.
2. Using forceps I tore the filters into small pieces and then ground them for 3 minutes in 90% acetone with a small (< 1 gram) amount of $MgCO_3$ added to it. After grinding, chlorophyll was extracted from samples in 90% acetone for less than 24 hours in a dark refrigerator.
3. Samples were removed from the refrigerator and allowed to warm to room temperature for 30 minutes. I then diluted the samples to 1 ml of sample: 7ml of 90% acetone, because the chlorophyll concentrations of the periphyton samples were much greater than those from the phytoplankton samples.
4. After dilution, chlorophyll-a concentrations of the samples were read using the fluorometer. After each initial reading I added three drops of 0.5 M HCL to acidify the sample and then placed the sample back in the fluorometer to determine pheophyton-a concentrations of the sample.
5. After collecting data from all samples I used the following formulae to determine chlorophyll-a and pheophyton-a concentrations in mg/m^2:

   Step 1:
   chlorophyll-a $\mu g/L = (r / r - 1) (R_b - R_a)$

   pheophyton-a $\mu g/L = (r / r - 1) (rR_a - R_b)$

*where:
r = 2.08 (before/after standard calibration)
R_b = sample reading before adding acid
R_a = sample reading after adding acid

Step 2:
(µg/L) x (L/m^2) = $µg/m^2$

*where:
µg/L = the value from *Step 1*
L/m^2 = total volume extracted for each tile in liters divided by the area of the tile in $meters^2$ (for this experiment L/m2 = 0.014/0.1016)

Step 3:
(0.001) x [the value from *Step 2* ($µg/m^2$)] = mg/m^2

Step 4:
[the value from *Step 3* (mg/m^2)] x (DF)

*where:
DF = dilution factor (the final volume divided by the diluent volume)

Appendix F

Musculature of the Chondrocranium

Table A-1. Origins and insertions of selected cranial muscles. Modified from Gradwell 1972.

Muscle	Origin	Insertion
	Mandibular Group	
Levator mandibulae posterior superficialis (lmps)	Dorsal part of the palatoquadrate	Dorsal, medial part of the Meckel's cartilage
L. m. p. profundus (lmpp)	Dorsal part of the palatoquadrate	Lateral part of the suprarostral cartilage
L. m. anterior (lma)	Dorsal part of the ascending process of the palatoquadrate	Dorsal, lateral part of the Meckel's cartilage
L. m. externus (lme)	Anterior part of the muscular process of the palatoquadrate	Lateral part of the suprarostral cartilage
L. m. a. articularis (lmaa)	Dorsal, lateral part of the palatoquadrate	Dorsal, lateral part of the Meckel's cartilage
L. m. a. subexternus (lmas)	Anterior, medial surface of the muscular process of the palatoquadrate	Lateral part of the suprarostral cartilage
Intermandibularis posterior	Median raphe	Median part of Meckel's cartilage
	Hyoid Group	
Hyoangularis (HA)	Lateral part of ceratohyal	Retroarticular process of Meckel's cartilage
Quadratoangularis (QA)	Inferior, lateral part of muscular process of palatoquadrate	Retroarticular process of Meckel's cartilage
Suspensorioangularis (SA)	Superior, lateral part of muscular process of palatoquadrate	Retroarticular process of Meckel's cartilage
Orbitohyoideus (OH)	Lateral part of muscular process of the palatoquadrate	Lateral part of ceratohyal
Suspensoriohyoideus (SH)	Posterior, lateral part of muscular process of the palatoquadrate	Lateral part of ceratohyal
Interhyoideus (IH)	Median raphe	Lateral part of ceratohyal

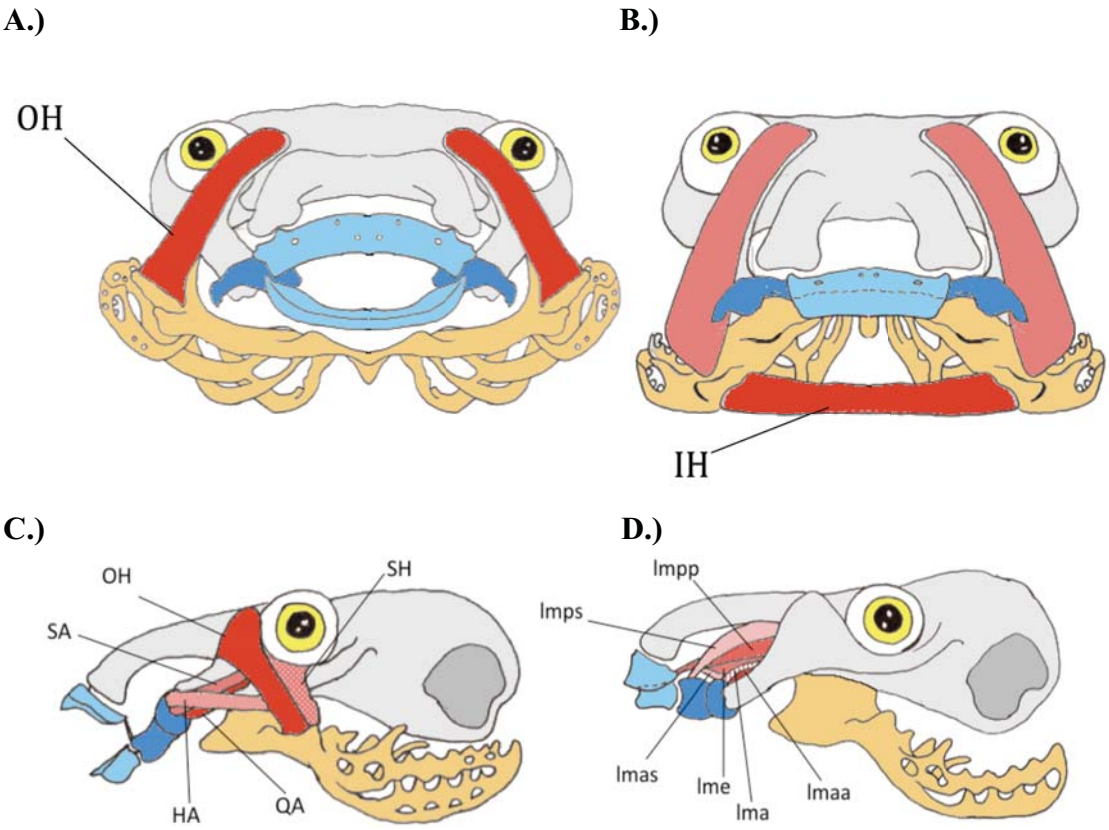

Figure A-1. Frontal view illustration of depression of the buccal floor during filter feeding (A), and elevation of the buccal floor during filter feeding (B). Lateral view illustration of jaw opening during rasping feeding (C), and jaw closing during rasping feeding (D). Abbreviations are listed in Table A-1.